C.P. No. 1291

C.P. No. 1291

LIBRARY
ROYAL AIRCRAFT ESTABLISHMENT
BEDFORD.

PROCUREMENT EXECUTIVE, MINISTRY OF DEFENCE

AERONAUTICAL RESEARCH COUNCIL

CURRENT PAPERS

Measurement of the Internal Performance of a Rectangular Air Intake Mounted on a Fuselage at Mach Numbers from 1.6 to 2

PART IV

by

C. S. Brown and E. L. Goldsmith

Aerodynamics Dept., R.A.E., Bedford

LONDON: HER MAJESTY'S STATIONERY OFFICE

1974

PRICE £1 NET

UDC 533.697.2 : 533.6.015 : 533.6.011.5 : 533.695.29

CP No.1291
June 1972

MEASUREMENT OF THE INTERNAL PERFORMANCE OF A RECTANGULAR AIR INTAKE MOUNTED ON A FUSELAGE AT MACH NUMBERS FROM 1.6 TO 2

Part IV

by

C. S. Brown
E. L. Goldsmith

CORRIGENDA

Corrections

Page 5 line 9 should read:-

... survey. The probes were 0.10in (2.54mm)

line 10 should read:-

... 60^{o}. Five orifices of 0.010in (0.254mm)

Page 6 line after equation (2) should read:-

where A_e is the maximum capture area

UDC 533.697.2 : 533.6.015 : 533.6.011.5 : 533.695.29

CP No.1291*
June 1972

MEASUREMENT OF THE INTERNAL PERFORMANCE OF A RECTANGULAR AIR INTAKE MOUNTED ON A FUSELAGE AT MACH NUMBERS FROM 1.6 TO 2

Part IV

by

C. S. Brown
E. L. Goldsmith

SUMMARY

A rectangular variable geometry intake, whose internal performance in a uniform flow field had previously been measured, has been tested on a fuselage. The intake has been tested with its leading edge both horizontal and vertical. In the case of the vertical intake, the effect of removing the lower swept endwall has been investigated.

The tests were done in a range of Mach number from 1.61 to 2.01 at incidences from 0° to 12°. The Reynolds number based on intake entry height was approximately 0.7×10^{6}.

This particular fuselage appears to impose only a small effect on the intake performance when the intake is horizontal. However a survey of the fuselage flow field indicates the complexity of the flow entering the intake and emphasizes the difficulty in using average flow properties to establish very accurate estimates of mass flow.

The vertical intake suffers considerable loss of performance both in terms of maximum mass flow and critical point pressure recovery at incidences above about 4° when fitted with swept endwalls. By removing the lower swept endwall, the zero incidence performance can be maintained up to incidences of 12°.

---

* Replaces RAE Technical Report 72136 - ARC 34333

CONTENTS

Negs. C 9277 to C 9278

1 INTRODUCTION

An extensive programme of wind tunnel tests has been carried out at RAE Bedford to investigate the internal performance of a particular rectangular intake both in a uniform flow field and on a fuselage.

The results of the tests on the isolated intake in a uniform flow field at Mach numbers from 1.7 to 2.5 are contained in Refs.1 and 2. This Report presents the results from tests in which the intake was installed on the side of a fuselage forebody and was operating in the flow environment generated by the nose and canopy. The intake has been tested with its leading edge horizontal, and also with its leading edge vertical as in a fuselage-side arrangement.

The forebody flow field was surveyed in the plane of the intake leading edge by means of a number of calibrated conical probes[3].

2 DESCRIPTION OF THE TEST RIG

Figs.1 and 2 show the intake, duct and forebody assembled on the General Intake Test Rig used in the 3ft × 3ft supersonic wind tunnel at RAE Bedford. This rig has been described in Ref.4. It consists of a sting support, a calibrated mass flow control and measuring unit, a hydraulic actuator system for moving the compression surface ramps and an instrumented duct with interchangeable exit plugs for controlling and measuring the intake bleed flow.

3 DETAILS OF THE MODEL

The intake model is that used in Refs.1 and 2. The ratio of height to width at the entry plane is 1.54 and the geometry of the compression surface ramps, cowl and bleed are as shown in Fig.3a. The first compression surface has a fixed angle δ_1 of 10° and the shock from its leading edge theoretically falls on the cowl lip at a free stream Mach number of 2.43. The second compression surface is movable and is linked to the rear ramp. In the configuration in which the intake leading edge is vertical, these two movable surfaces are connected to the hydraulic actuator system on the intake test rig. However when the intake is assembled on the fuselage so that its leading edge is horizontal this arrangement is not possible and the movable surfaces, although still linked together in the manner shown in Fig.3a, are controlled by means of a manually operated lead screw.

The gap between the second and rear ramps forms a slot for bleeding the boundary layer from the compression surfaces and this slot extends over the

whole width of the intake. The geometry of the bleed exit is shown in Fig.4. Although a number of interchangeable plugs of different exit area are available, the data in the present series relate to tests which were done with a constant bleed exit area equal to 10 per cent of the intake entry area.

Two different shapes of endwall were used in these tests. One is the so-called swept endwall in which the leading edge coincides with the line joining the leading edge of the intake to the cowl lip. The other is a minimal endwall, which is sufficient to contain the space under the second compression surface at maximum δ_2, but otherwise has a leading edge which is vertical at the cowl lip. Details of the two shapes are shown in Fig.3b and some idea of the difference between them when assembled can be obtained from Figs.2a and 2b.

The area distribution through the intake and duct for various values of δ_2 is shown in Fig.5. The ratio of engine face cross-sectional area to maximum capture area is 0.88 and the distance from the cowl lip to the engine face is 9.89 times the intake height.

The nose and canopy only of the fuselage are represented. Fig.6 gives details of the forebody including the relationship between the fuselage datum, the intake datum and the nose cone centre line. The model is mounted in the tunnel on the intake datum line so that α_∞ is the angle of incidence of the intake relative to the wind tunnel free stream. Fig.6 also indicates the location on the fuselage of the intake in both the horizontal and vertical positions and the locations of the yawmeters and pitot rakes used to survey the fuselage flow field.

3.1 Instrumentation

The standard mass flow control and measuring unit[4] is fitted with a cruciform rake having a total of 24 pitot tubes for measuring total pressure at the engine face station. The tubes are disposed for area-weighted averaging and the rake is rotatable to enable pressure surveys to be made in greater detail. Static pressure at the engine face is measured by using four holes equally spaced round the circumference. Additionally static pressure is measured in the venturi section of the mass flow unit, downstream of the engine face rake; and this pressure is monitored and used in the on-line computation of performance characteristics.

The bleed duct contains twelve pitot tubes for measuring total pressure and three holes for measuring static pressure arranged as shown in Fig.4.

A single rake of six pitot tubes was used to measure the pressure distribution on the centre line of the intake at the entrance to the fixed portion of the subsonic diffuser.

The instrumentation for the fuselage flow field survey consisted of four rakes each containing three conical probes, which were calibrated to give local pressure recovery, Mach number and flow inclination; and six pitot tubes to provide a boundary layer pressure survey. The probes were 0.01in (0.254mm) diameter cones with an included angle of 60°. Five orifices of 0.10in (2.54mm) diameter were located on each cone; one at the nose to measure pitot pressure and four on the conical surface spaced at 90° intervals. The sign convention adopted to define flow inclination is indicated on Fig.6.

4 DETAILS OF THE TESTS

4.1 Test conditions

The tests were all done in the 3ft × 3ft tunnel and the table below lists the tunnel free stream Mach numbers M_{∞} and Reynolds numbers based on intake entry height (R_e) at which the various configurations were tested.

	Endwall shape	M_{∞}	α_{∞}°	δ_2°	R_e
Intake leading edge horizontal	Both endwalls swept	1.70	0, 2½, 5, 7½, 10	0, 5, 7, 9	0.694×10^6
		1.81	0, 2½, 5, 7½, 10	0, 5, 7, 9	0.670×10^6
		2.01	0, 2½, 5, 7½, 10	2, 5, 7, 9	0.565×10^6
Intake leading edge vertical	Both endwalls swept	1.60	0, 4, 8, 12	0	0.785×10^6
		1.81	0, 4, 8, 12	0	0.730×10^6
		2.01	0, 4, 8, 11	5	0.565×10^6
	Both endwalls unswept	1.60	0, 4, 8, 12	0	0.785×10^6
		1.81	0, 4, 8, 12	0	0.730×10^6
		2.01	0, 4, 8, 11	5	0.565×10^6
	Upper endwall swept: Lower endwall unswept:	1.60	0, 4, 8, 12	0	0.785×10^6
		1.81	0, 4, 8, 12	0	0.730×10^6

4.2 Data reduction

In the case of the fuselage flow field investigation, calibration data obtained with the conical probes and the five pressure measurements on each cone provided sufficient information for calculating the local Mach number, total pressure and flow angularity for each probe location in the flow field. The data reduction procedure was based on Ref.4.

In the combined intake-fuselage investigation the test technique was that described in Ref.1. Pressure recovery-mass flow ratio characteristics for both the engine and the bleed ducts were measured for each model configuration at the values of M_∞, δ_2 and intake incidence listed in the table in section 4.1.

Pressure recovery is defined as

$$\frac{P_f}{P_\infty} \quad \text{or} \quad \frac{P_B}{P_\infty} = \frac{1}{nP_\infty} \sum_1^n P_j \tag{1}$$

where P_∞ is the free stream total pressure

and P_j is the pitot pressure at the jth tube in the rake at the engine face station in the case of P_f or in the rake in the bleed duct in the case of P_B, and n is the number of pressure points in the survey.

Mass flow ratio in both engine and bleed ducts was calculated assuming the exit flows to be choked:-

$$\left(\frac{A_\infty}{A_e}\right) = \frac{P}{P_\infty} \frac{A_{ex}}{A_e} \left(\frac{A}{A^*}\right)_\infty \tag{2}$$

where A_e is the maximum captive area

and A_{ex} is the effective choked exit area as determined by calibration in the case of the engine duct. In the case of the bleed duct the exit was not calibrated and A_{ex} was taken to be the geometric bleed exit area

$\frac{P}{P_\infty}$ is either the engine face pressure recovery $\frac{P_f}{P_\infty}$ or the bleed duct pressure recovery $\frac{P_B}{P_\infty}$

$\left(\frac{A}{A^*}\right)_\infty = (1 + 0.2M_\infty^2)^3/1.728M_\infty$.

4.3 Accuracy

Errors in the direct measurement of engine face and bleed duct total pressure and therefore in pressure recoveries based on free stream total pressure are thought to be small; not more than 0.1 per cent. However uncertainty in the value of mean M_∞ obtained from the wind tunnel calibration and in the value of the effective choked area obtained from the calibration of the mass flow measuring unit probably means that the error in mass flow ratio could be as much as half a per cent.

The accuracy of the reduced test data from the flow field survey is difficult to quantify.

5 DISCUSSION OF RESULTS

5.1 Survey of fuselage flow field

The calculations of local Mach number, total pressure and flow angularity for each probe location in the flow field, obtained from the calibration data together with the five pressure measurements on each cone, are shown in Figs.7 to 10, plotted against α_∞ the angle of incidence of the intake datum line, for free stream Mach numbers M_∞ of 2.01 and 1.81. Immediately obvious is the complexity of the flow environment in which the intake is operating, and the difficulty in attributing mean values to the properties of the stream entering the intake. In an attempt to relate the performance of the intake in the environment generated by the forebody to its performance in a uniform flow field, the local properties given by the twelve probes have simply been averaged arithmetically. These averages, which are shown in Figs.7 to 10, have been adopted as the mean properties for the purpose of the analysis in section 5.2.2.

Results of the boundary-layer survey are shown in Figs.11 and 12 for free stream Mach numbers of 2.01 and 1.81 and for a number of angles of incidence of the intake datum line. These indicate that the intake is always clear of the fuselage boundary layer.

5.2 Intake mounted on the fuselage with its leading edge horizontal

5.2.1 General

Internal performance characteristics for the intake when mounted on the fuselage with its leading edge horizontal, are shown in Figs.13, 14 and 15 for free stream Mach numbers M_∞ of 2.01, 1.81 and 1.70. Engine face pressure recovery is shown plotted against total mass flow, bleed mass flow and bleed

pressure recovery. A constant relationship exists between bleed recovery and bleed mass flow at each Mach number because the bleed exit area is constant and the bleed exit is always choked.

The emphasis in the analysis of these characteristics is on the comparison between the intake performance on and off the fuselage. Earlier parts of this Report[1,2] contain a detailed analysis of shock patterns, the effect of internal contraction etc., as intake free stream Mach number, second wedge angle and angle of incidence of the intake are varied, which in general is also relevant to the present results.

5.2.2 Comparison of installed performance with the performance of the isolated intake

(i) Direct comparison at M_∞ = 1.70 and 2.01

In Figs.16, 17, 18 and 19 the performance of the installed intake as expressed by maximum total mass flow and critical point pressure recovery is compared directly with the performance of the isolated intake[2] at the same free stream Mach number and the same inclination of the free stream relative to the intake datum, for free stream Mach numbers of 1.70 and 2.01. At first sight there would seem to be large areas of agreement. However there are some noticeable discrepancies, in particular in mass flow at M_∞ = 2.01 at both low and high incidences and in pressure recovery at both Mach numbers at high incidence. These are thought to be significant and in the next section an attempt is made to compare measured results for the intake on the fuselage with measured results for the isolated intake taking into account the local flow conditions measured on the fuselage.

(ii) Isolated intake results adjusted for fuselage flow field

(a) Mass flow

Maximum mass flow for the intake on the fuselage can be represented as:-

$$\left[\frac{A_\infty}{A_e}\right]^F_{(M,\alpha)_\infty} = \frac{P_f}{P_\infty}\left(\frac{A}{A^*}\right)_\infty \frac{A_{ex}}{A_e} \qquad (3)$$

$$= \frac{P_L}{P_\infty}\frac{(A/A^*)_\infty}{(A/A^*)_L}\frac{P_f}{P_L}\left(\frac{A}{A^*}\right)_L \frac{A_{ex}}{A_e}$$

$$= \lambda\left[\frac{A_\infty}{A_e}\right]^A_{(M,\alpha)_L} \qquad (4)$$

measured results on the installed intake and the measured results on the isolated intake when adjusted for the body flow field are very good except at α_∞ equal to 10^o and values of δ_2 where the second oblique shock is well detached.

In Fig.23 some complete pressure recovery-mass flow characteristics for the intake installed on the fuselage and in isolation are compared for various angles of incidence of the fuselage datum at $M_\infty = 2.01$. The isolated intake characteristics have been adjusted by means of the parameters $(\lambda\psi)$ and $(\phi\theta)$ to take account of the fuselage flow field. It is clear that although critical flow values of both pressure recovery and mass flow agree well, with the exceptions referred to above; when the intake operates increasingly sub-critically, differences in pressure recovery of 0.01 to 0.03 develop. Moreover these differences are opposite in sign for δ_2 of 5^o and 9^o; and no adequate explanation can be given.

(iii) Installed performance at $M_\infty = 1.81$

Maximum mass flow and pressure recovery at critical flow conditions for the intake when installed on the fuselage at $M_\infty = 1.81$ are shown in Figs.24 and 25. The measured data is compared with calculations based on shock patterns and adjusted for local flow conditions and at $\alpha_\infty = 0^o$ with data for the isolated intake taken from Ref.1. Measured maximum mass flow compares very well with the estimates at this Mach number, the discrepancy at $\delta_2 = 0^o$ for incidences of 5^o and above is due to the over-contraction of the duct causing failure of the intake to start and could have been predicted as indicated in Ref.2.

Fig.25 indicates losses other than shock losses for the installed intake slightly higher than would be suggested by adjustment of the isolated intake data for the effect of the body flow field.

5.2.3 Stable flow range and flow distortion at the engine face

The variation of stable flow range and of distortion coefficient DC_{60} with second ramp angle δ_2 are both shown in Figs.26, 27 and 28 for Mach numbers of 2.01, 1.81 and 1.70. Calculations of stable flow range have been made for Mach numbers of 2.01 and 1.81 in accordance with the method of Ref.5 using local flow conditions at the intake and these are included in Figs.26 and 27. Data for the isolated intake at Mach numbers of 2.01 and 1.70 have been taken from Ref.2 and repeated in Figs.26 and 28. Comparison at these

latter Mach numbers of the two sets of measured data indicates very little difference in the behaviour of the intake in the fuselage flow field to that in isolation. The results confirm the evidence of Ref.2 that where the second oblique shock is attached the method of Ref.5 appears to predict the stable flow range with fair success, but where a two shock system exists the method is less successful. In particular the results indicate a progressive increase of stable flow range with δ_2 and incidence up to the point at which the first oblique shock detaches after which the stable flow range appears to reach a constant maximum value of about 50 to 60 per cent.

No attempt has been made to adjust the measured installed DC_{60} values to allow for the distortion in the free stream over the area of the capture plane of the intake. It is interesting to note however that except at $\alpha_\infty = 10^\circ$ this 'free stream distortion' does in fact result in slightly less distortion at the engine face than was measured with the uniform free stream.

5.3 Intake mounted on the fuselage with its leading edge vertical

The performance characteristics for the intake when mounted on the fuselage with its leading edge vertical are shown in Figs.29, 30 and 31 where engine face pressure recovery is plotted against total mass flow and bleed pressure recovery. Data is presented for free stream Mach numbers of 1.61 and 1.81 with the intake second ramp angle δ_2 constant at 0°. Tests were made with three different combinations of top and bottom endwalls as indicated in Fig.3b. At $M_\infty = 2.01$ tests were done with $\delta_2 = 5^\circ$ using only those combinations of endwalls in which both endwalls were swept and both endwalls were unswept.

5.3.1 Maximum mass flow

The variation of maximum total mass flow ratio with intake incidence for the different configurations of endwall for Mach numbers of 1.61, 1.81, and 2.01 are shown in Fig.32. At Mach numbers of 1.81 and 2.01 maximum mass flow has been calculated from shock patterns using the average value of local Mach number obtained from the fuselage flow field survey, and these mass flow curves are indicated for comparison. This comparison reveals very significant losses in maximum mass flow and this mass flow deficit, i.e. the difference between measured and calculated values, has been plotted in Fig.33.

With both endwalls swept the deficit at zero incidence can be accounted for by the sidewash β_L in the flow entering the intake which would correspond

to an incidence of approximately -1^{o} in the case of a horizontal intake. Above an incidence of about 4^{o} the mass flow deficit increases very rapidly with incidence probably due to separation at the lower swept endwall. With both endwalls unswept (configuration 2) the deficit at zero incidence is significantly greater due to the outflow than can now take place particularly downstream of the second oblique shock[6]. However the mass flow deficit for this configuration remains practically constant with incidence within the range of incidence of the data. Separation which took place at the lower swept endwall is no longer so serious as the leading edge of the endwall is now effectively unswept.

At $M_{\infty} = 1.81$, the configuration with the top endwall swept and the lower endwall unswept (configuration 3) shows a gradual reduction, with incidence, in the mass flow deficit. This probably stems from the fact that the lower endwall is effectively downstream of the leading edge of the top endwall and when the intake is pitched it can accept an increasingly wider streamtube.

In Fig.34 the maximum engine face mass flow is shown for the different endwall configurations of the vertical intake and data from the horizontal intake are also included. Comparison of the various configurations suggests that the horizontal intake suffers less from the effect of incidence than the vertical intake except perhaps at large incidence (greater than 8^{o}) and where the vertical intake has its lower endwall unswept.

5.3.2 Pressure recovery

Pressure recovery at critical flow conditions for the various configurations of the vertical intake are shown plotted against intake incidence in Fig.35. At Mach numbers of 1.81 and 2.01 shock recoveries for the vertical intake calculated for a leading wedge angle of 11^{o} are included as are the measured data for the horizontal intake. The effect of the swept lower endwall in the case of the vertical intake is again apparent in the marked fall off in pressure recovery at incidences above about 4^{o}. Reducing both endwalls leads to a lower pressure recovery due to increased shock loss[6] although recovery is less seriously affected by incidence. However reducing the lower endwall only, while incurring little penalty at zero incidence is least affected by incidence.

Losses other than shock losses appear to be similar for all configurations so that at low incidence, up to about 5^{o} the horizontal intake with its higher theoretical shock recovery has some advantage. However at high incidences the vertical intake is probably better provided the lower endwall is not swept.

5.3.3 Stable flow range and flow distortion at the engine face

The variation of stable flow range and distortion coefficient DC_{60} with intake incidence is shown in Fig.36 for the various configurations of the vertical intake at Mach numbers 1.61, 1.81 and 2.01 and for values of δ_2 of 0°, 0° and 5° respectively. Where the data from the horizontal intake are available these are included. The stable flow ranges for the vertical intake are in general consistent with the Ferri criterion of the vortex sheet impinging on the cowl lip causing the onset of instability[5]. When the intake is horizontal the second oblique shock becomes detached at incidence. This form of instability then no longer exists and stable flow ranges become significantly greater. In the case of the vertical intake stable flow range appears to be little affected by incidences up to 12°.

There is some evidence of large values of DC_{60} occurring in the vertical intake at both $M_\infty = 1.81$ and $M_\infty = 2.01$ at high incidence. Otherwise at these Mach numbers DC_{60} remains fairly consistent in the region -0.2 to -0.3. There is however a noticeable increase in distortion coefficient at $M_\infty = 1.61$. It was not possible in these tests to make an extensive survey of the pressure distribution within the intake and it is possible that some distortion effects are masked by the mixing which must take place in the long duct.

6 CONCLUSIONS

A rectangular variable geometry intake whose internal performance has been measured in a uniform flow field has been tested on the side of a fuselage and operating in the flow environment generated by the nose and canopy. The intake has been tested with its leading edge both horizontal and vertical; and in the vertical configuration three different combinations of top and bottom endwalls were used.

The tests were done in a range of Mach numbers from 1.61 to 2.01 at incidences from 0° to 12°. The Reynolds number based on intake entry height was approximately 0.7×10^6.

A survey of the fuselage flow field indicates the complexity of the flow entering the intake and emphasizes the difficulty in using average flow properties to establish accurate estimates of mass flow and pressure recovery.

For this particular fuselage the effect of the reduced Mach number through the nose shock appears to be offset by the effect of upwash over quite a large proportion of the incidence range investigated. The fuselage flow field

thus imposes only a small effect on the intake performance except near zero incidence and at incidences above about 8^{o}, when the intake is horizontal. Within the range of incidence of the tests, the horizontal intake appears to suffer less from the effect of incidence than the vertical intake.

The performance of the vertical intake with both endwalls swept falls off very sharply at all Mach numbers in terms of both maximum mass flow and critical point pressure recovery when the incidence is above about 4^{o}. However by reducing the lower endwall so that its leading edge is no longer swept and is effectively downstream of the leading edge of the upper endwall, the zero incidence performance can be maintained up to an incidence of about 12^{o}.

NOTATION

A	cross-sectional area
$\left(\frac{A_\infty}{A_e}\right)$	mass flow ratio
CL	cowl lip shock detaches
DC_{60}	distortion parameter $= \frac{(P_f)_{minimum} - (P_f)_{mean}}{(\frac{1}{2}\rho V^2)_f}$
h	height of intake leading edge above fuselage surface
M_∞	free stream Mach number
M_L	local Mach number behind fuselage nose shock
$\frac{P_f}{P_\infty}$	engine face pressure recovery
$\left(\frac{P_f}{P_\infty}\right)_c$	engine face pressure recovery at critical flow conditions
$\frac{P_B}{P_\infty}$	bleed duct pressure recovery
P_∞	free stream total pressure
P_L	local total pressure behind fuselage nose shock
P_P	pitot pressure in fuselage boundary-layer survey
SFR	stable flow range
SO	second oblique shock detaches
V	velocity
y	height of boundary-layer survey pitot above fuselage surface
X	distance downstream of cowl lip
α_∞	inclination of free stream relative to intake datum
α_L	inclination of flow behind fuselage nose shock relative to intake datum
δ_1	first compression surface angle relative to intake datum
δ_2	angle between first and second compression surfaces
β_L	angle of sideslip of flow downstream of fuselage nose shock
ρ	density

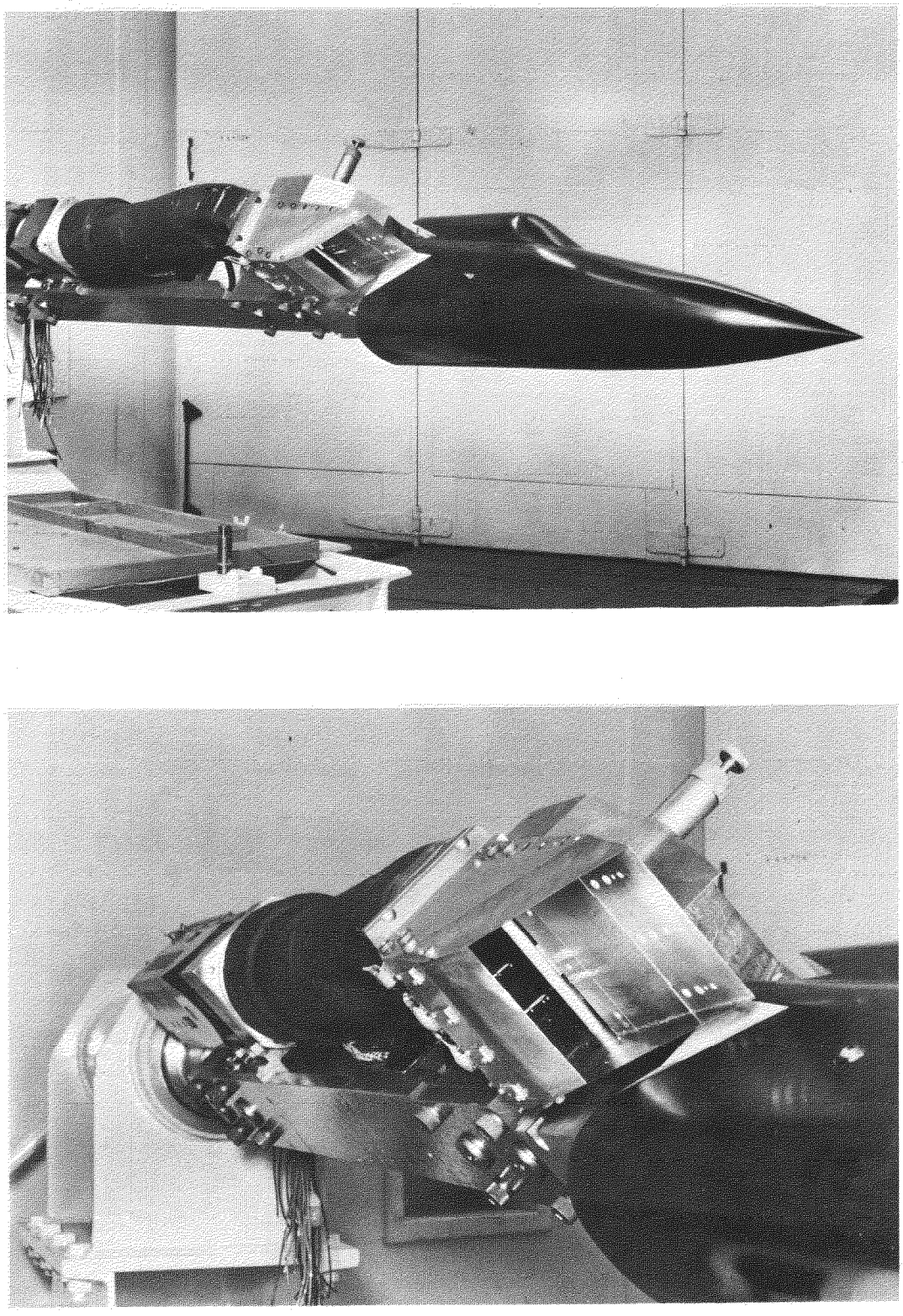

Fig.1 Intake, duct and airflow meter assembled with fuselage on intake test rig. Intake leading edge horizontal

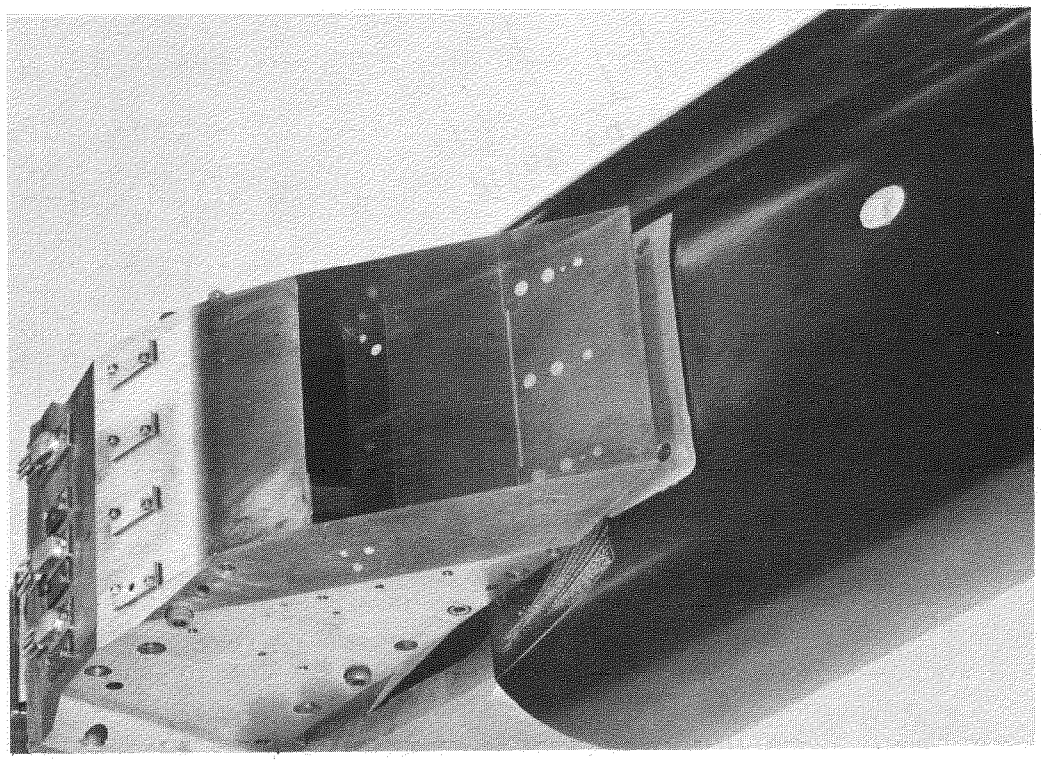

Fig.2a Intake on fuselage with intake leading edge vertical and both endwalls swept

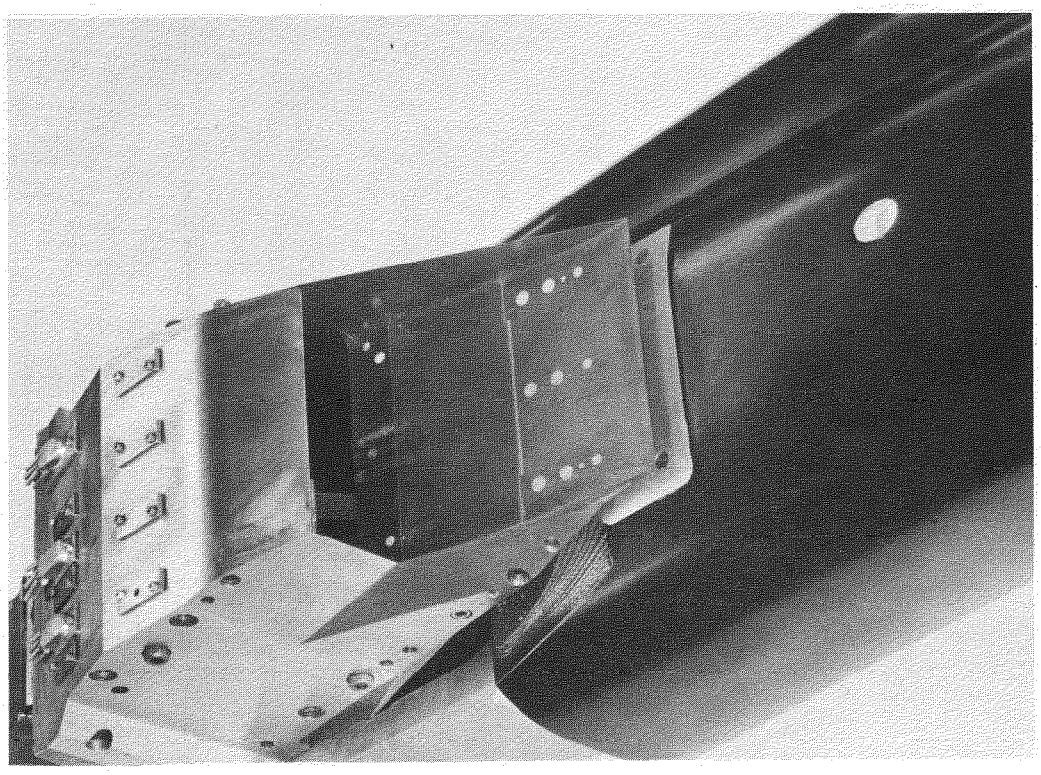

Fig.2b Intake on fuselage with intake leading edge vertical. Upper endwall swept and lower endwall unswept

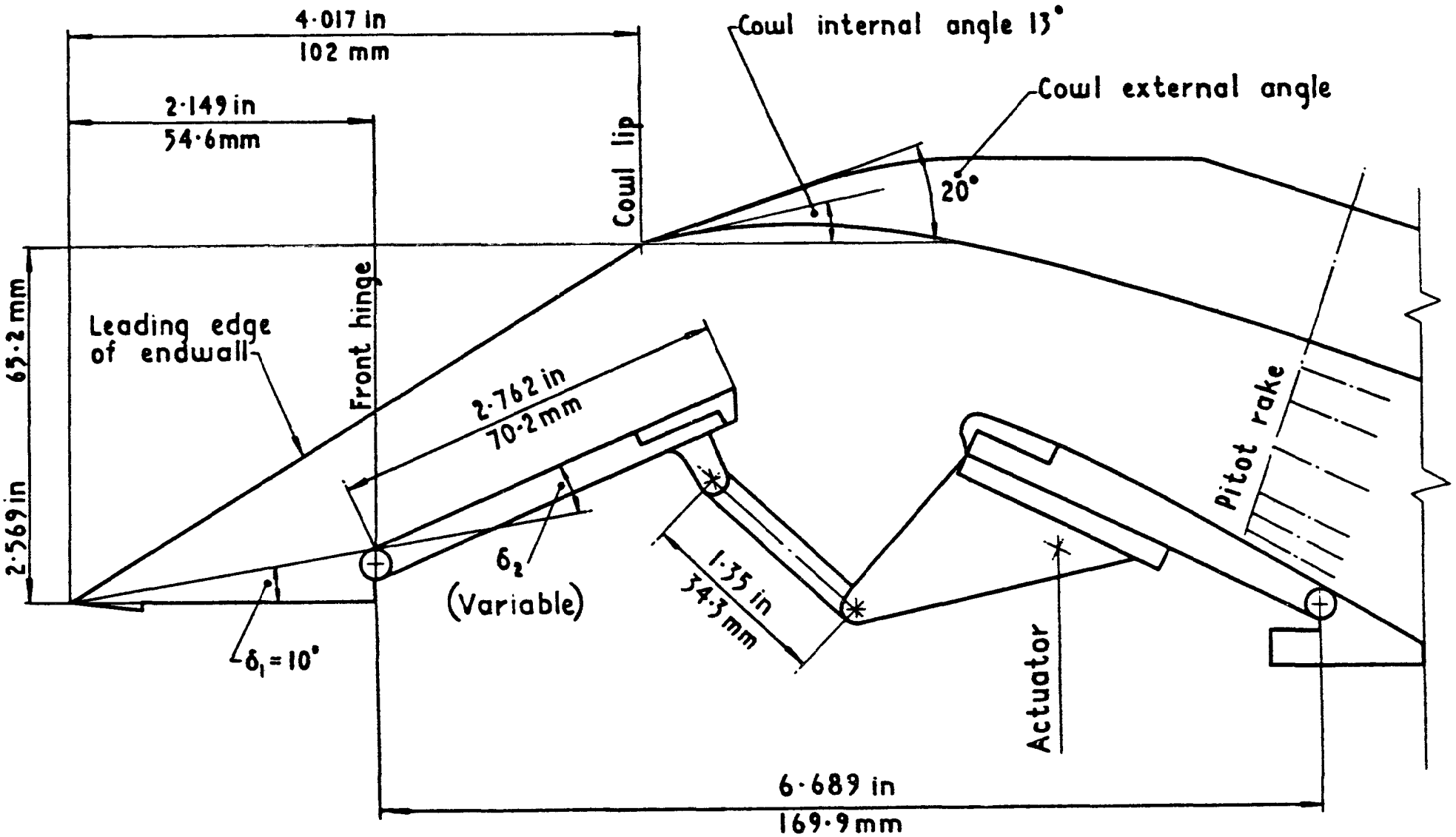

Fig.3a Geometry of compression surface ramps, cowl and bleed

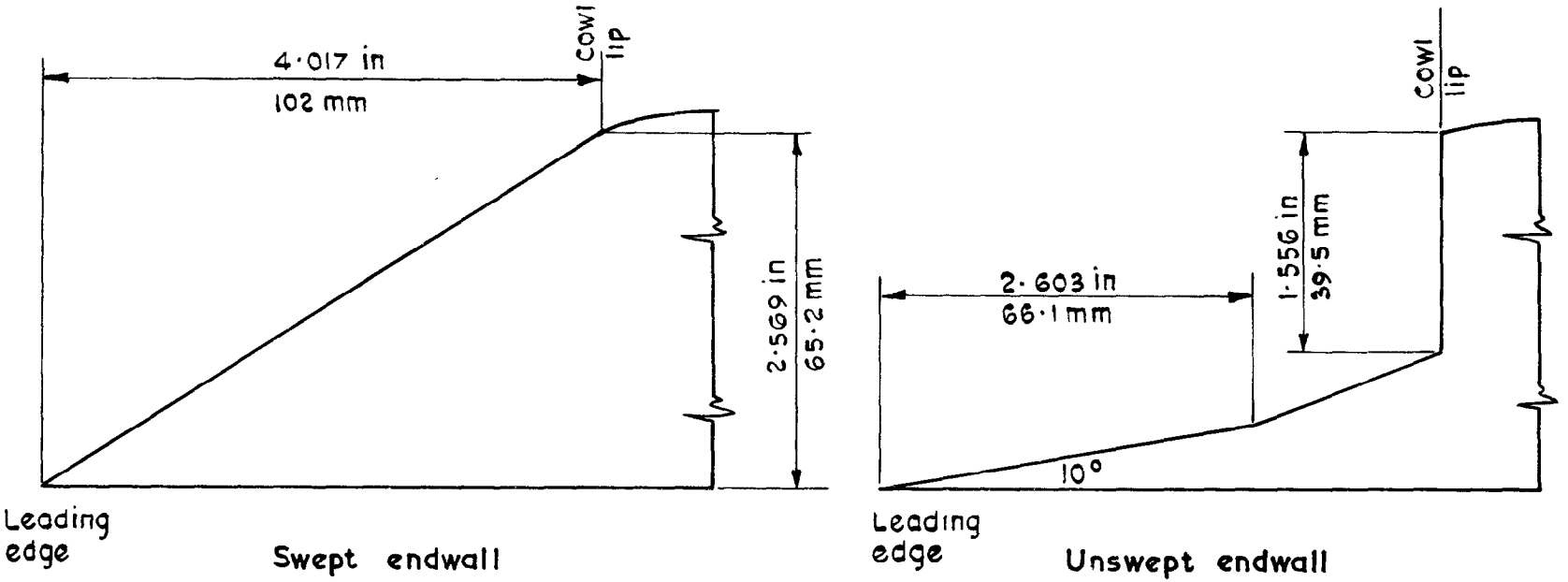

Configuration	Top Endwall	Bottom Endwall
1	swept	swept
2	unswept	unswept
3	swept	unswept

Fig. 3b Details of endwalls & endwall configurations

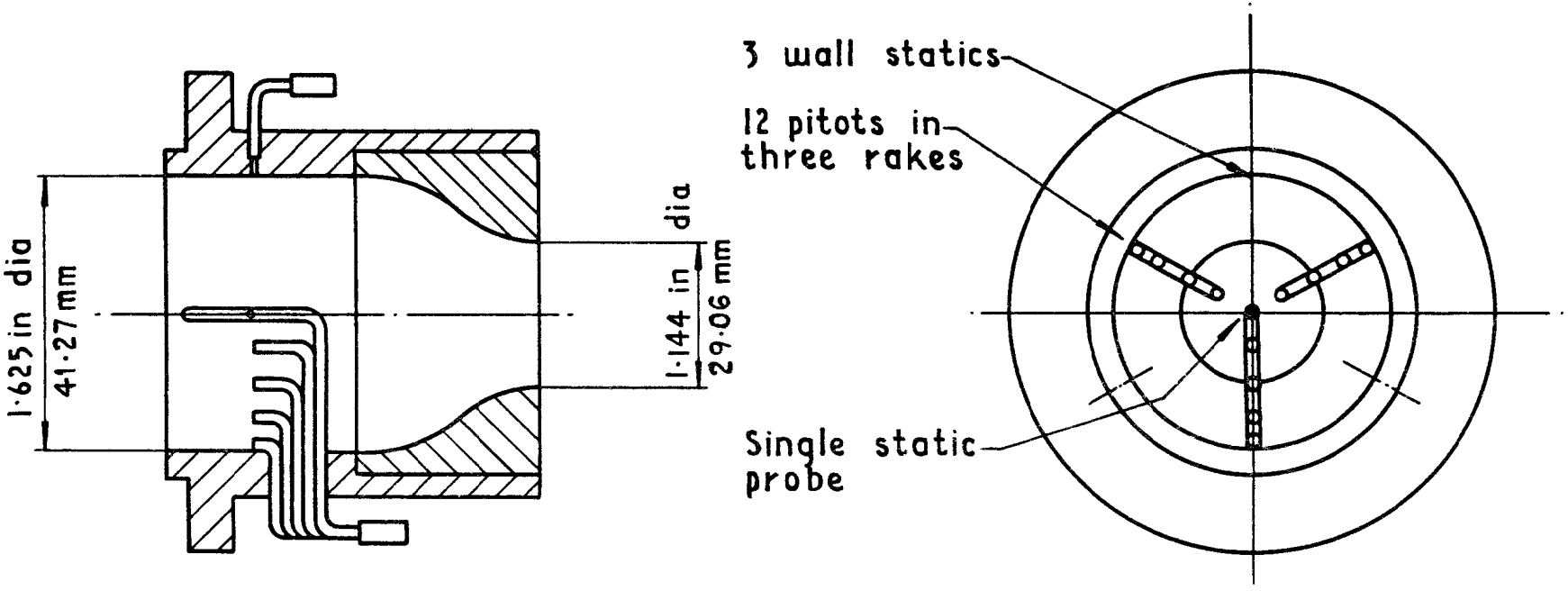

Fig.4 Details of bleed instrumentation and bleed exit plugs

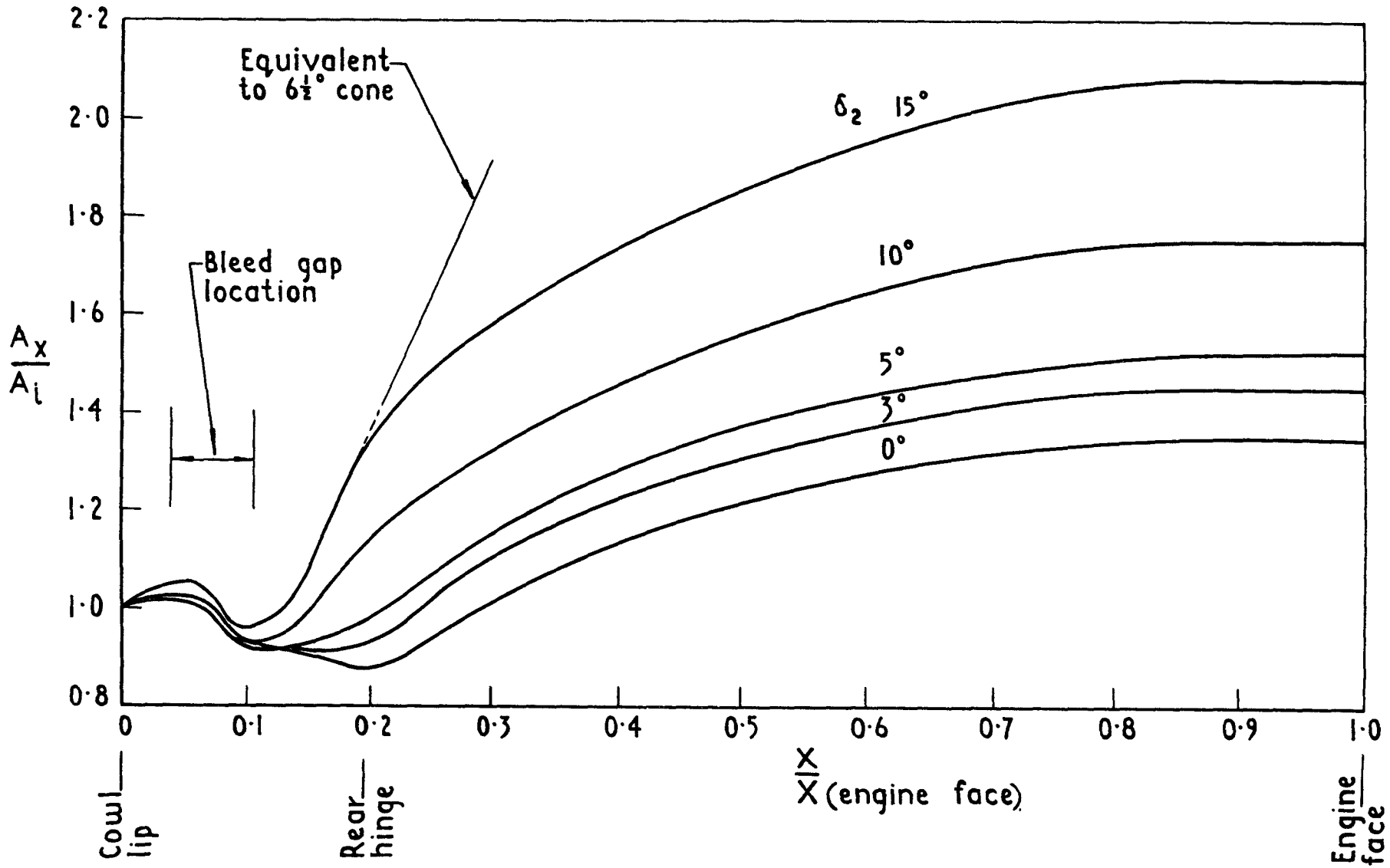

Fig.5 Area distribution through intake and duct

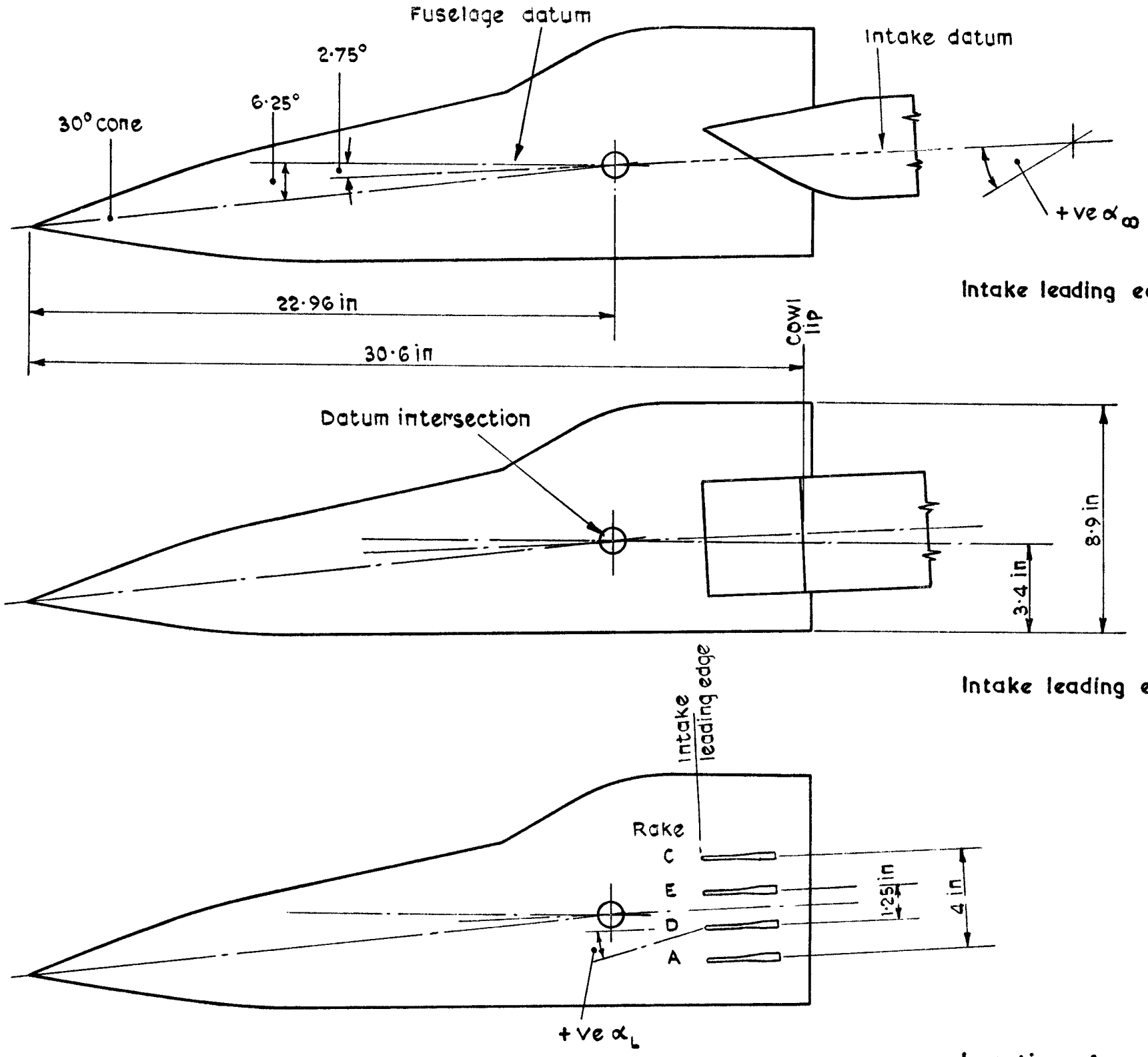

Intake leading edge horizontal

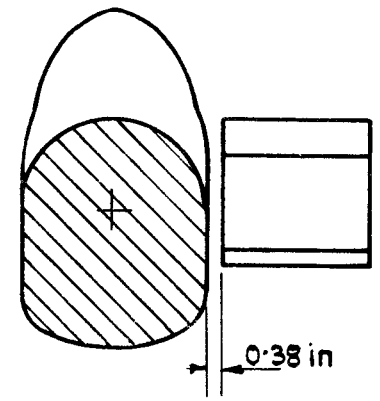

Intake leading edge vertical

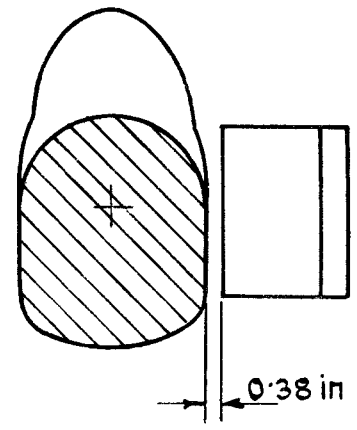

Location of yawmeters

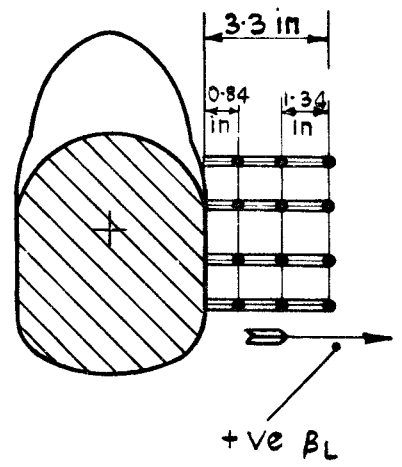

Fig. 6 Details of fuselage showing location of intake & yawmeters

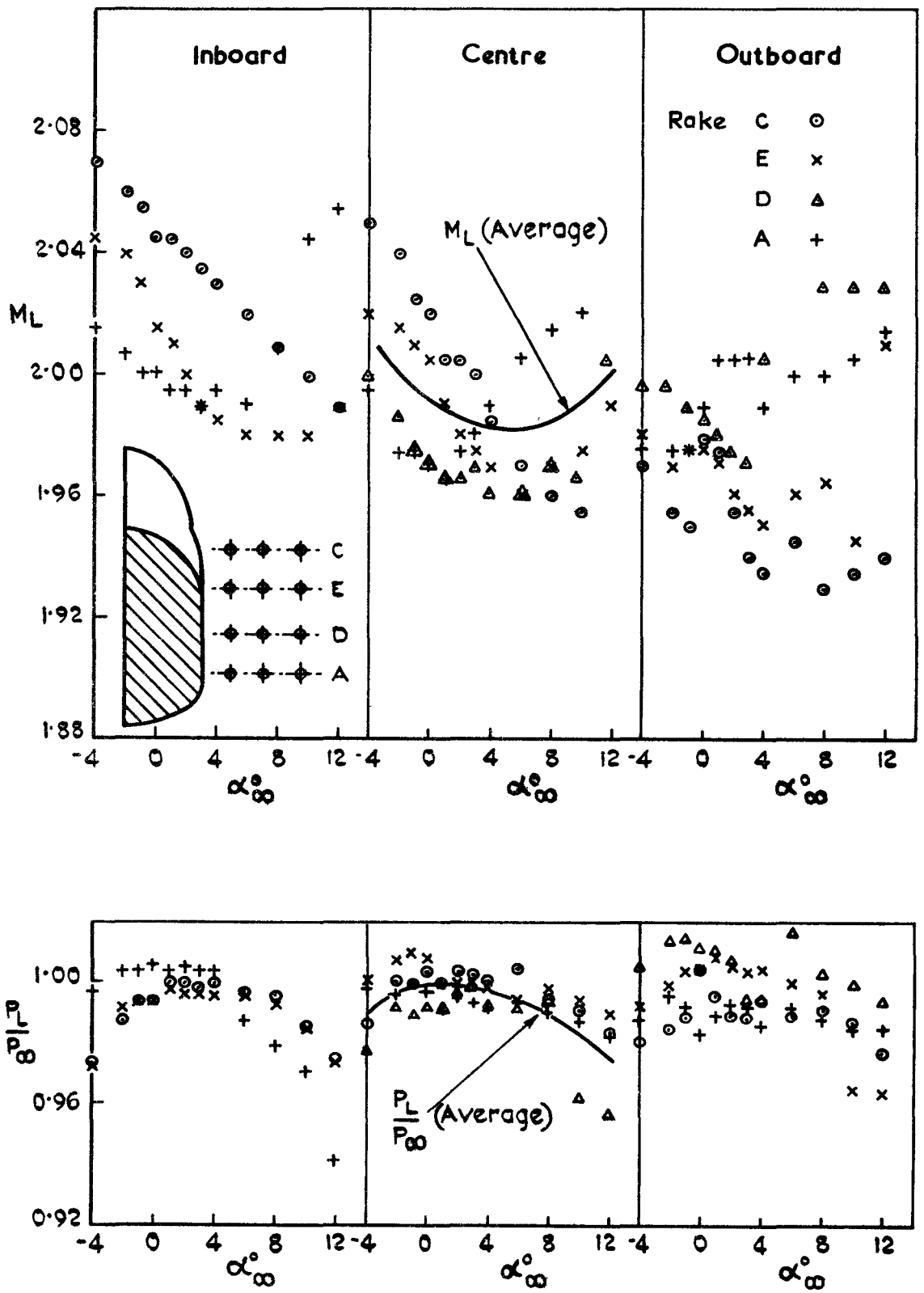

Fig. 7 Local Mach No & total pressure.
Fuselage flow field. M_∞ 2·01

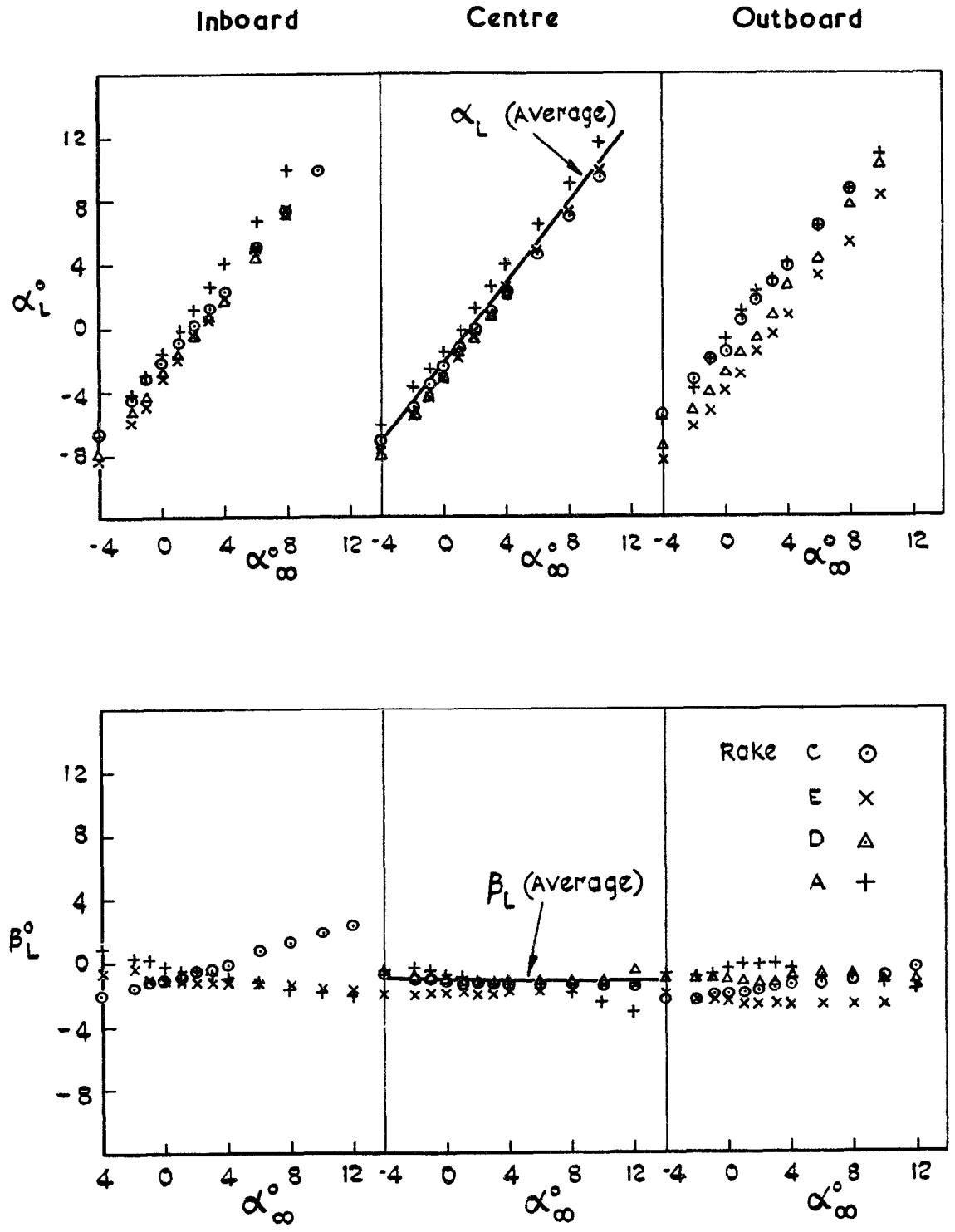

Fig.8 Local flow inclination.
Fuselage flow field M_∞ 2·01

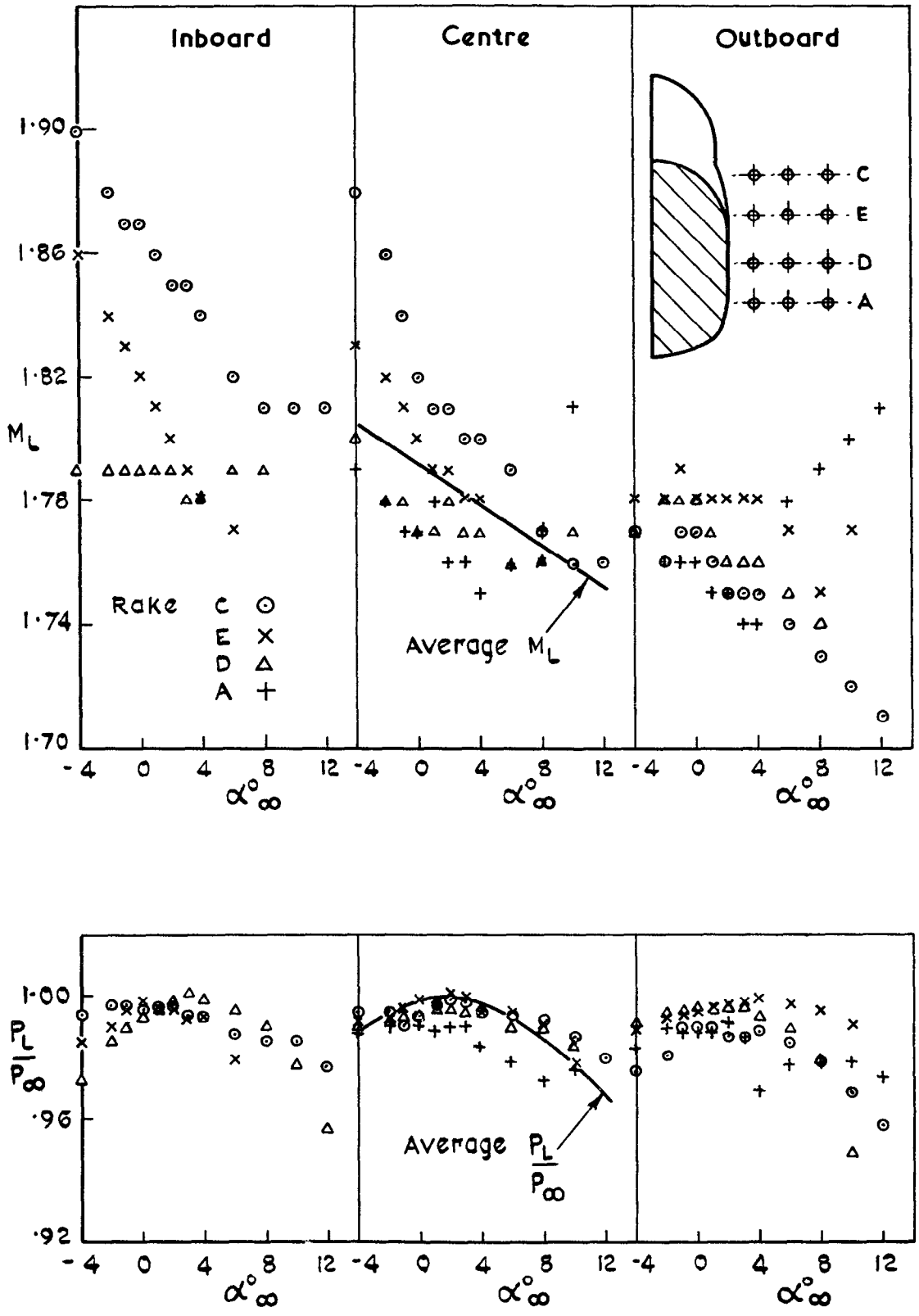

Fig. 9 Local Mach No & total pressure.
Fuselage flow field M_∞ 1·81

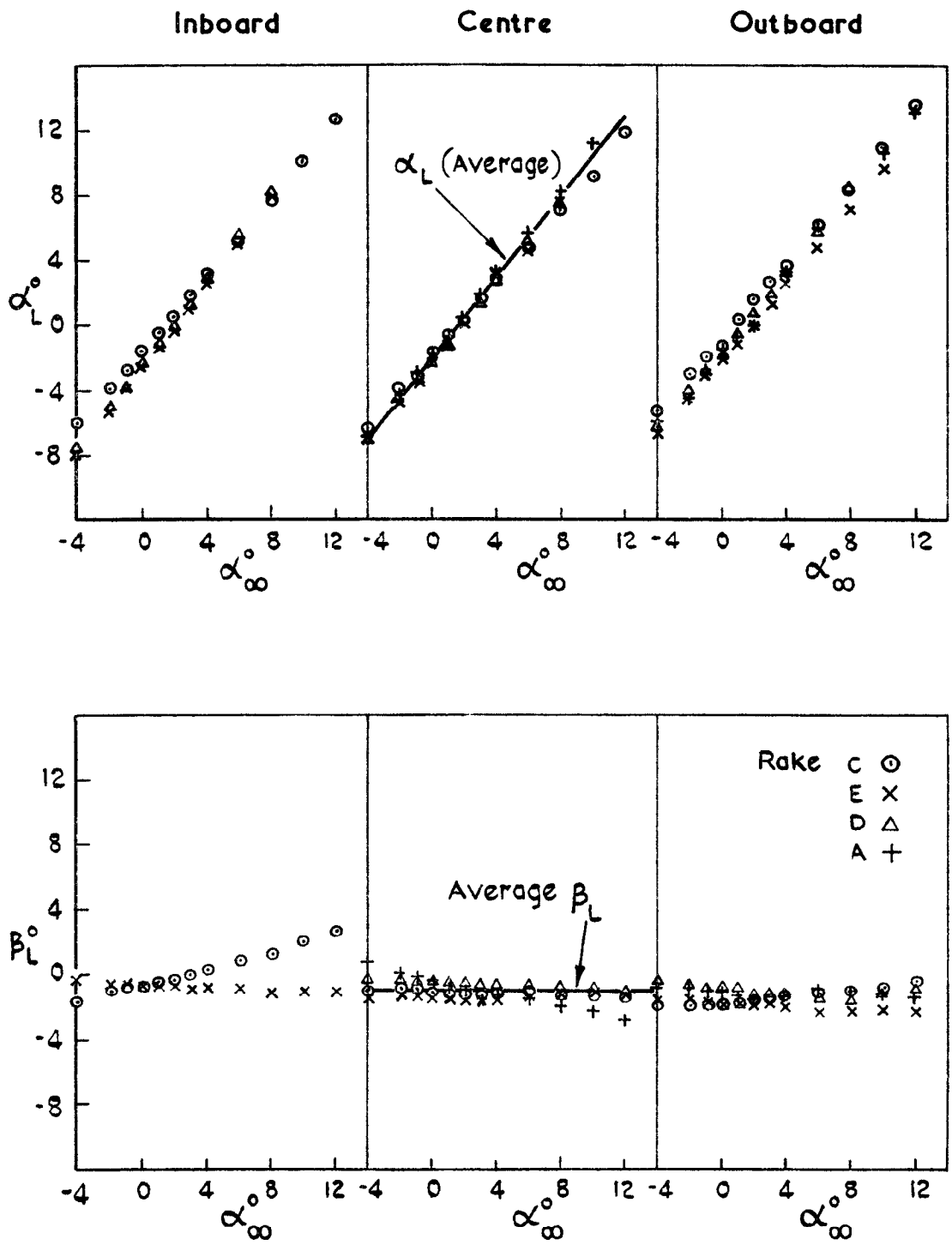

Fig.10 Local flow inclination.
Fuselage flow field M_∞ 1·81

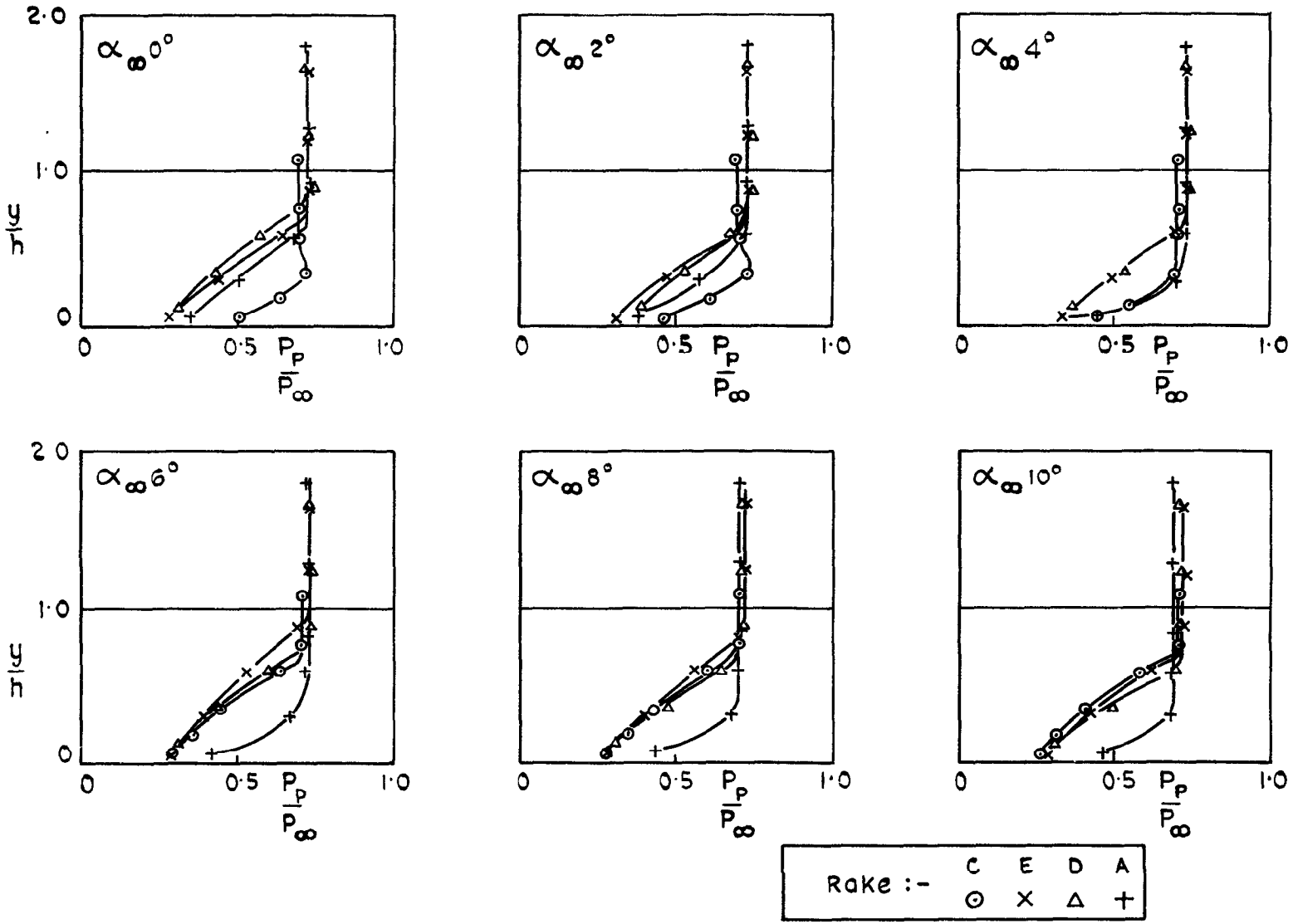

Fig.11 Pressure distribution on fuselage surface at leading edge of intake

M_∞ 2·01

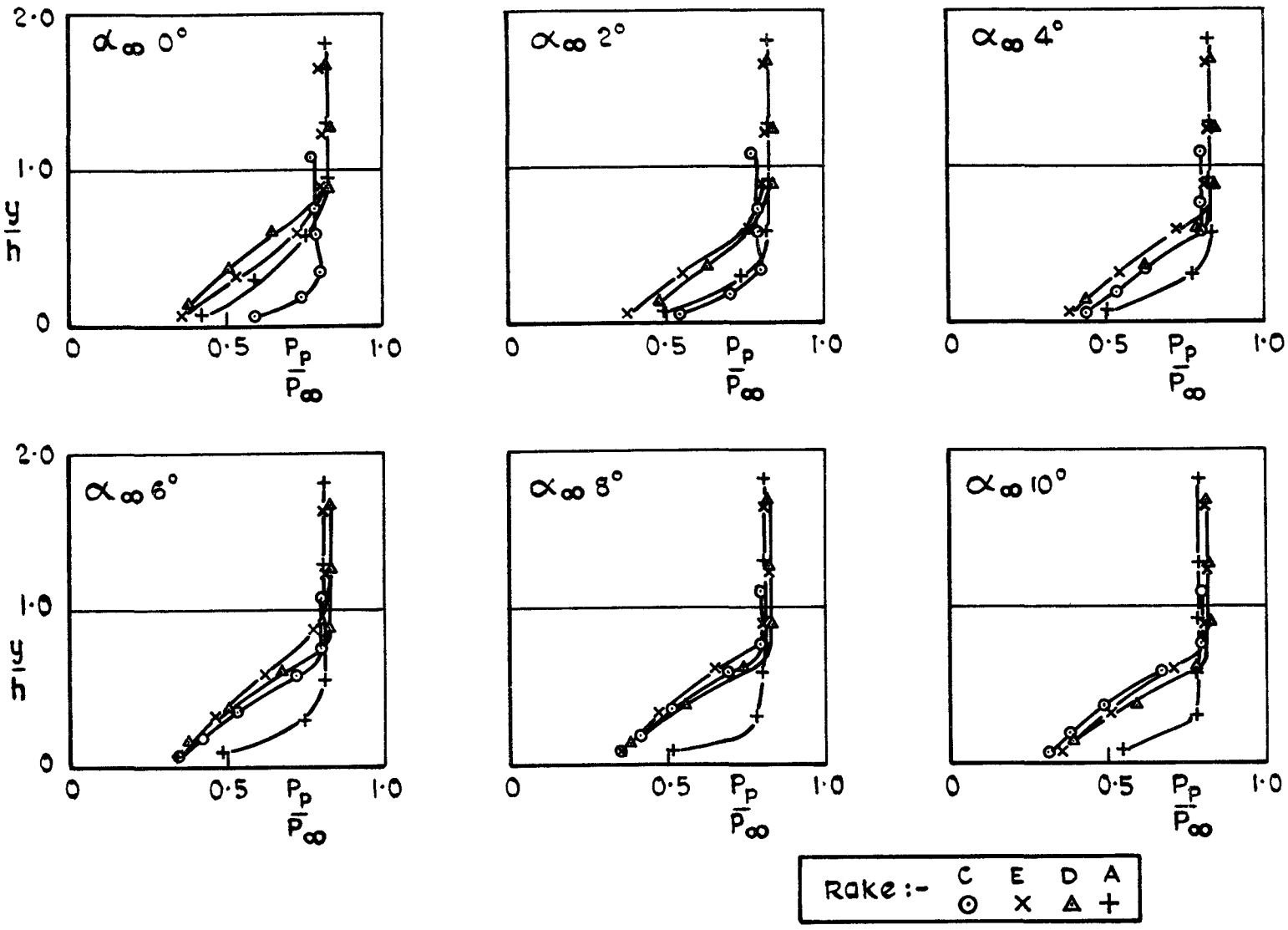

Fig. 12 Pressure distribution on fuselage surface at leading edge of intake. M_∞ 1·81

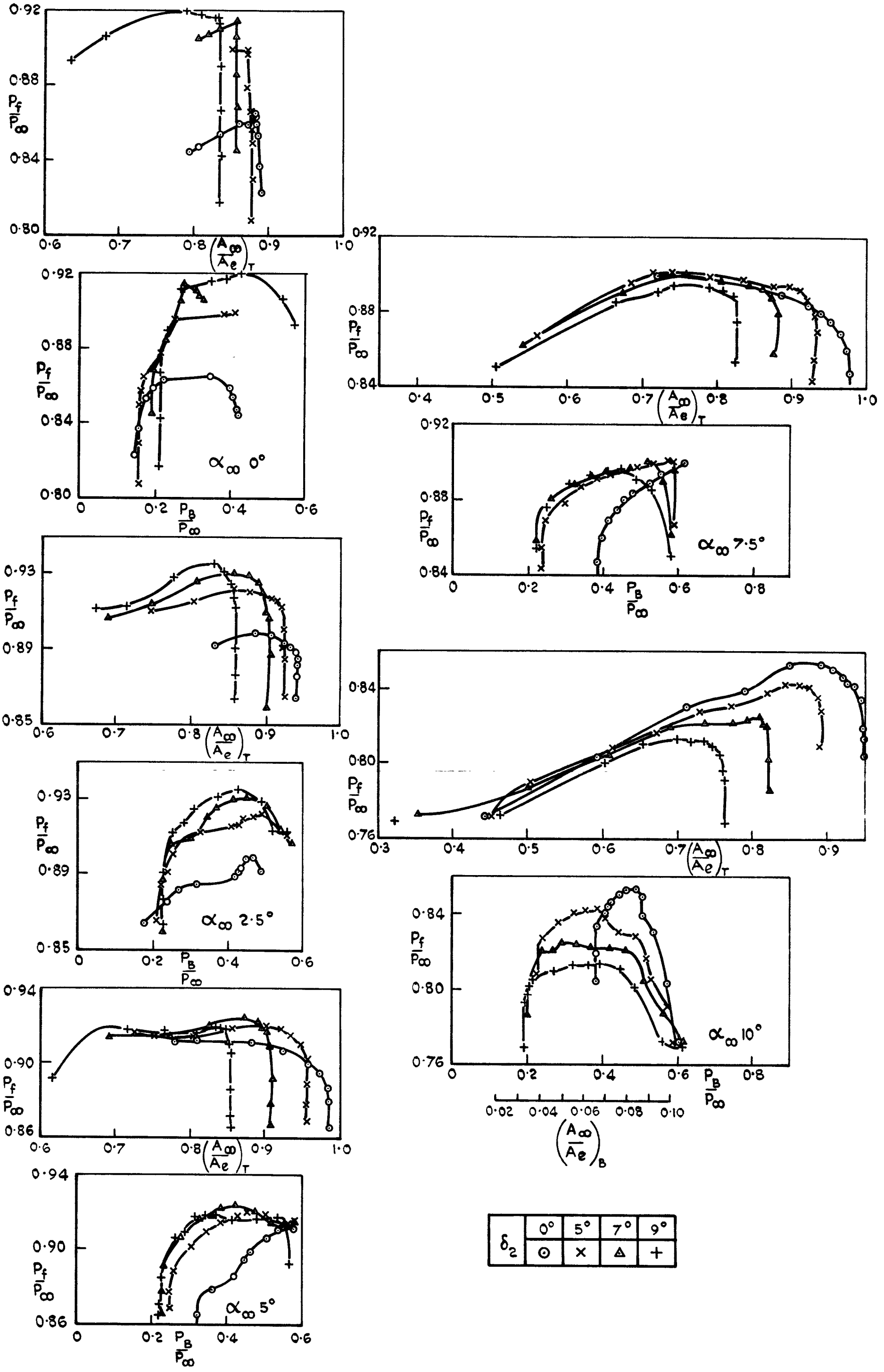

Fig.13 Variation of engine face pressure recovery with total mass flow and bleed pressure recovery – intake horizontal – M_∞ 2·01

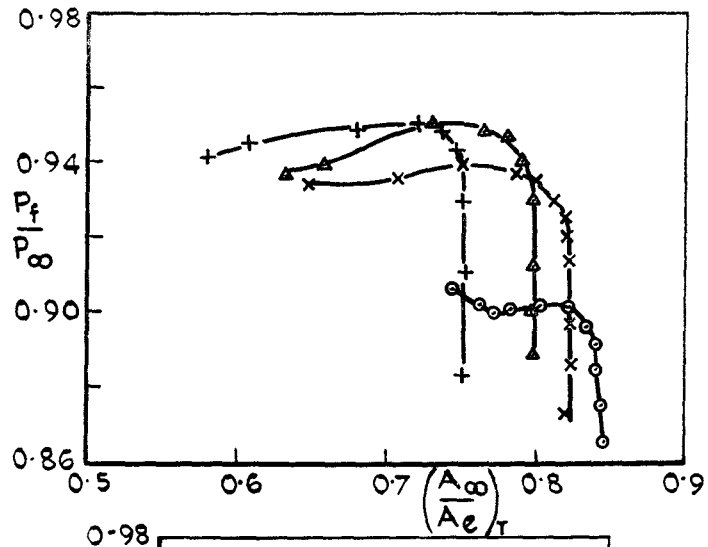

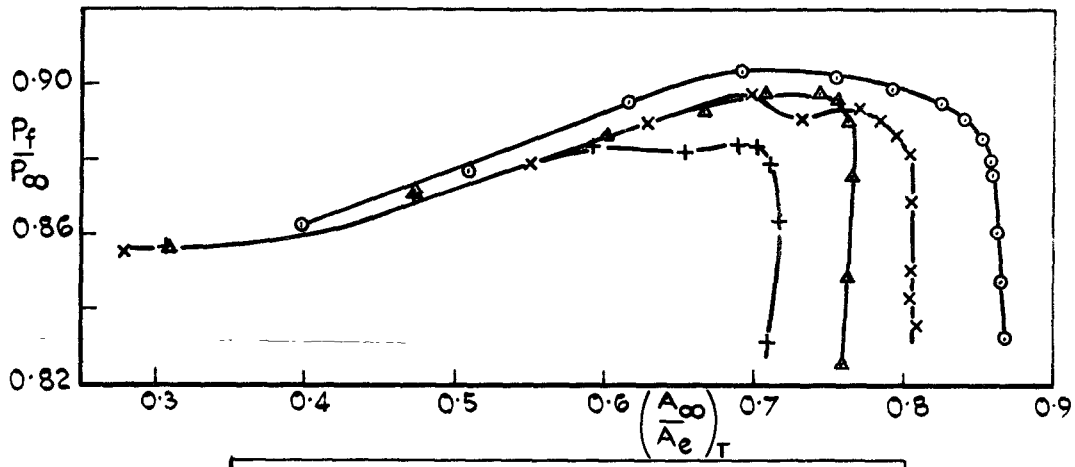

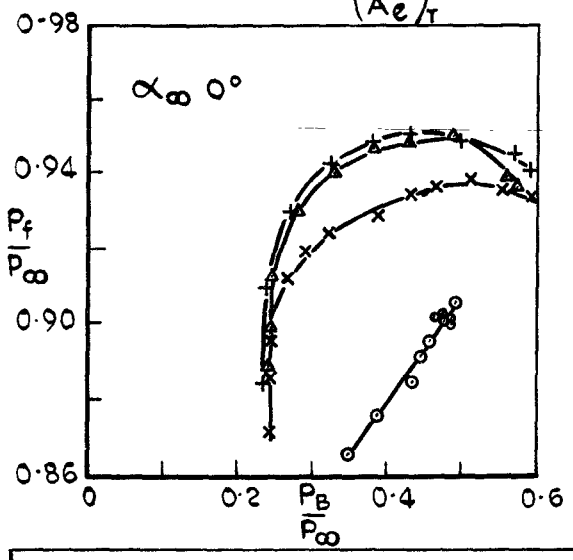

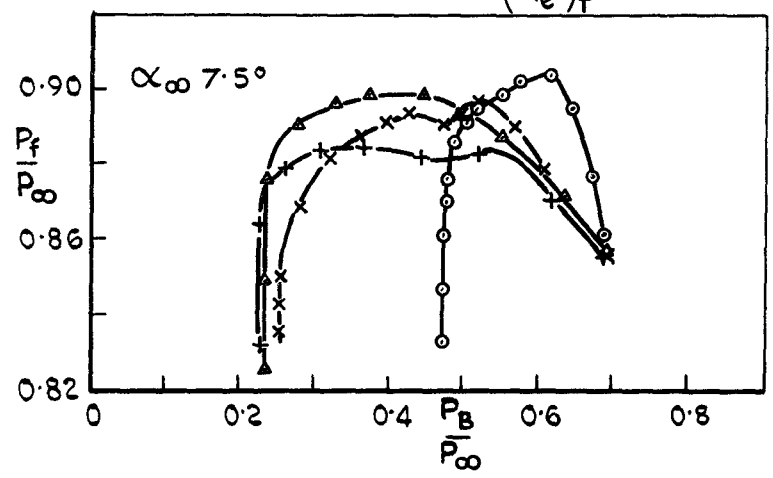

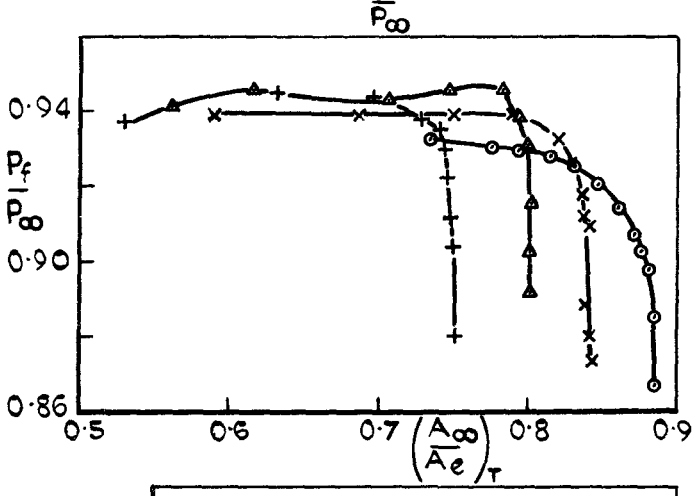

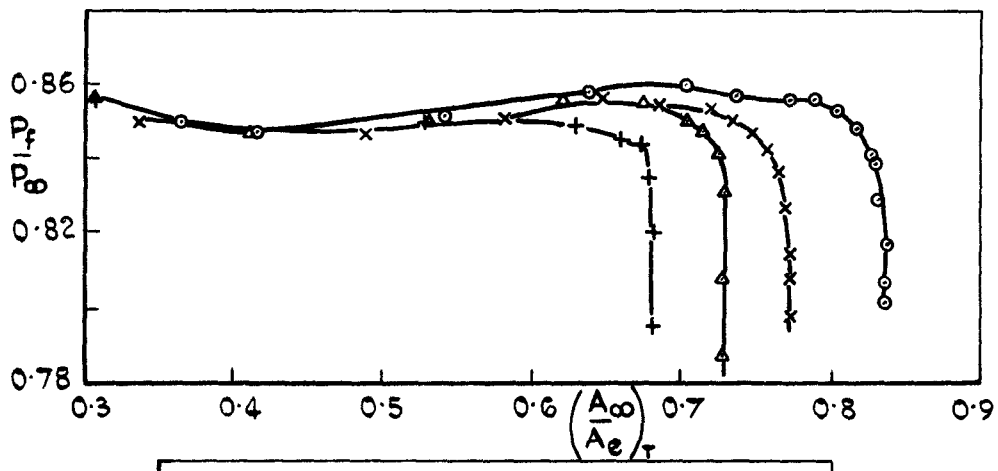

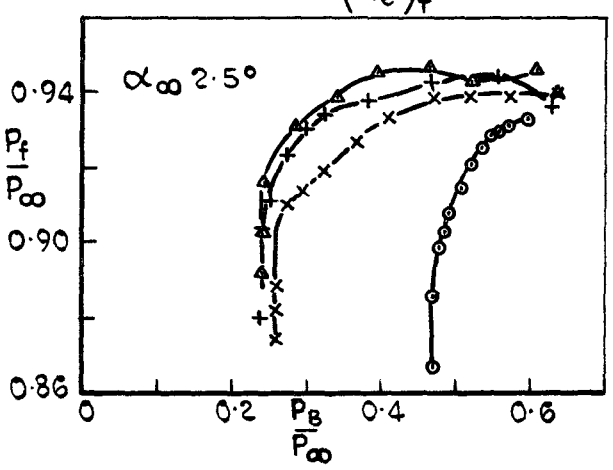

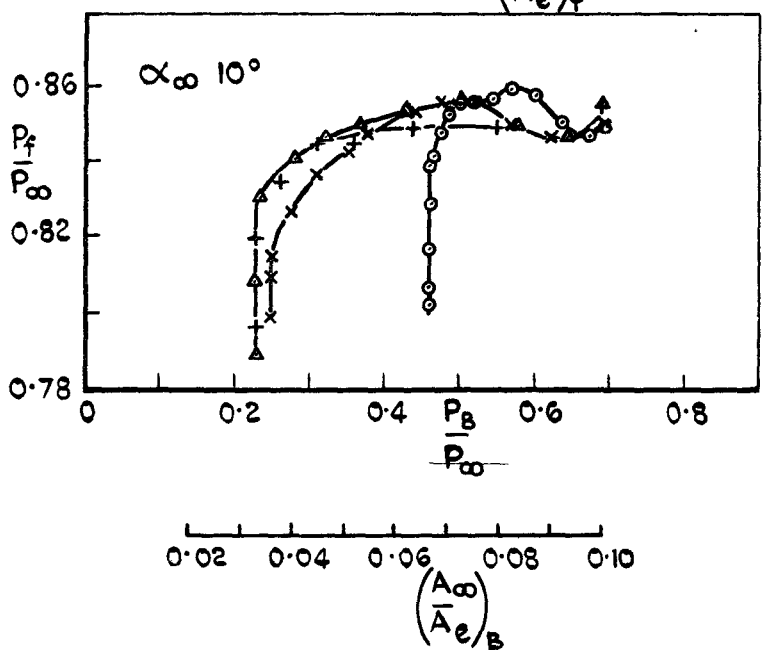

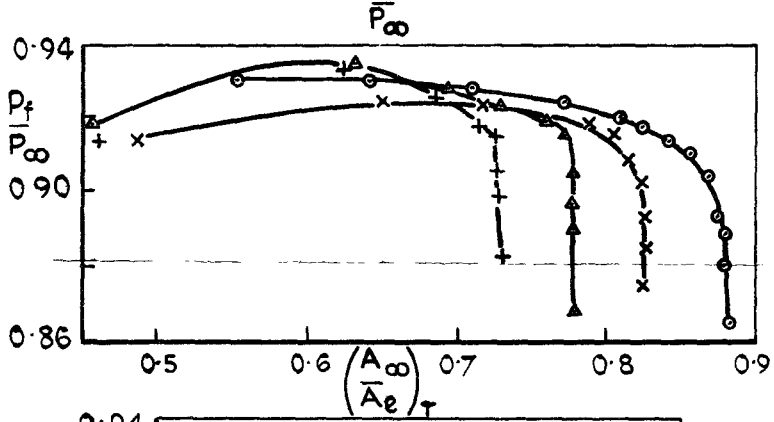

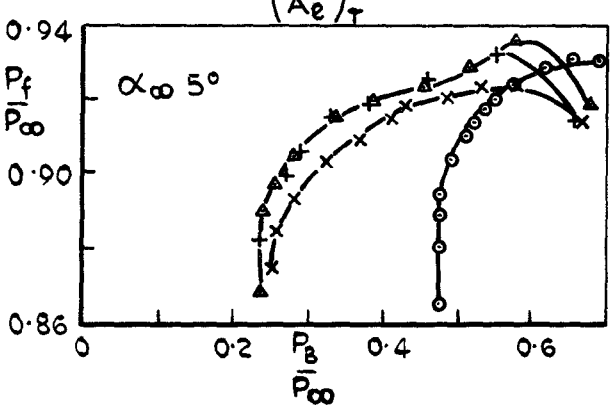

δ_2	0°	5°	7°	9°
	⊙	×	△	+

Fig.14 Variation of engine face pressure recovery with total mass flow & bleed pressure recovery —— Intake horizontal —— M_∞ 1·81

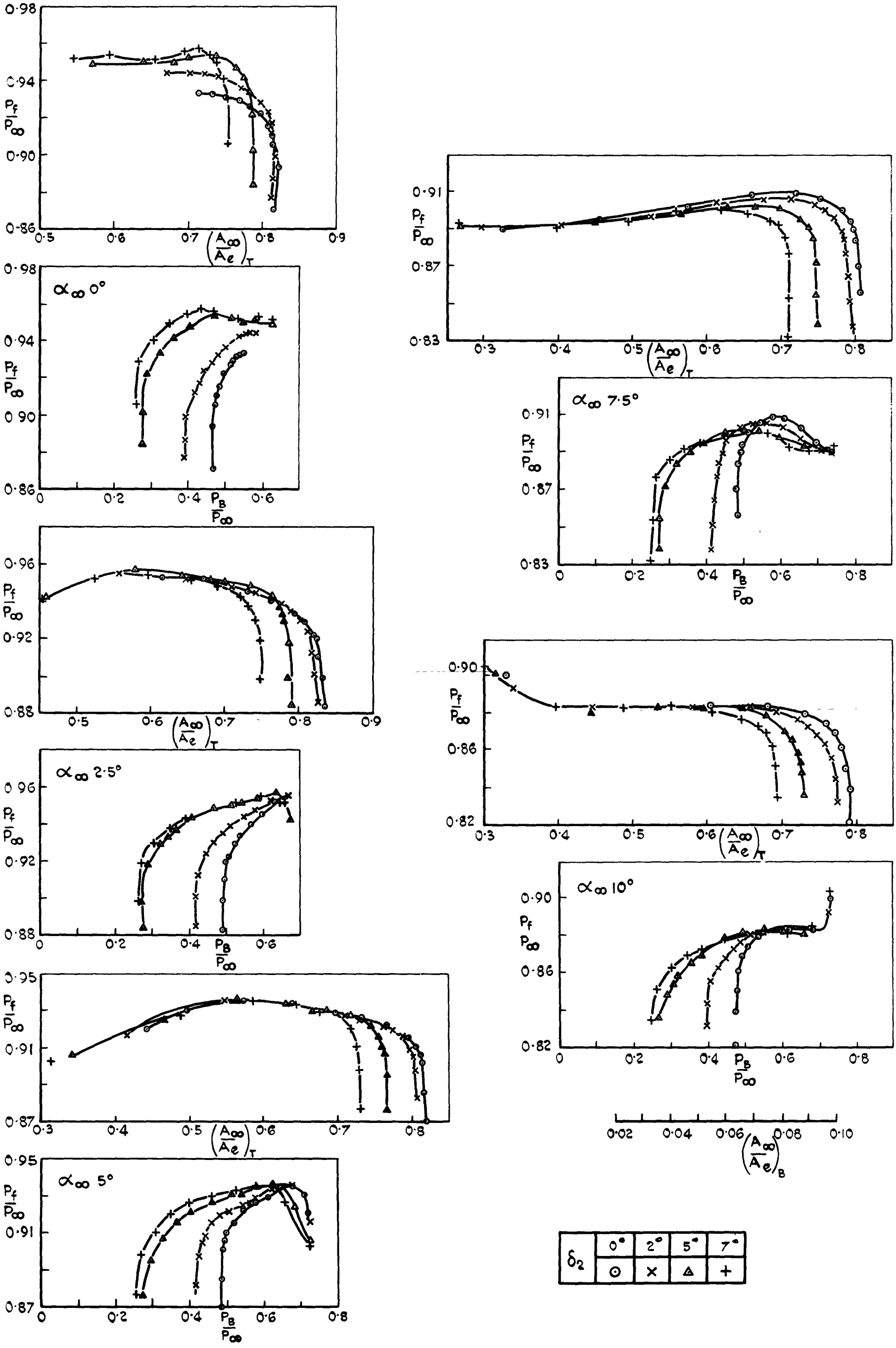

Fig.15 Variation of engine face pressure recovery with total mass flow and bleed pressure recovery – intake horizontal – M_∞ 1·70

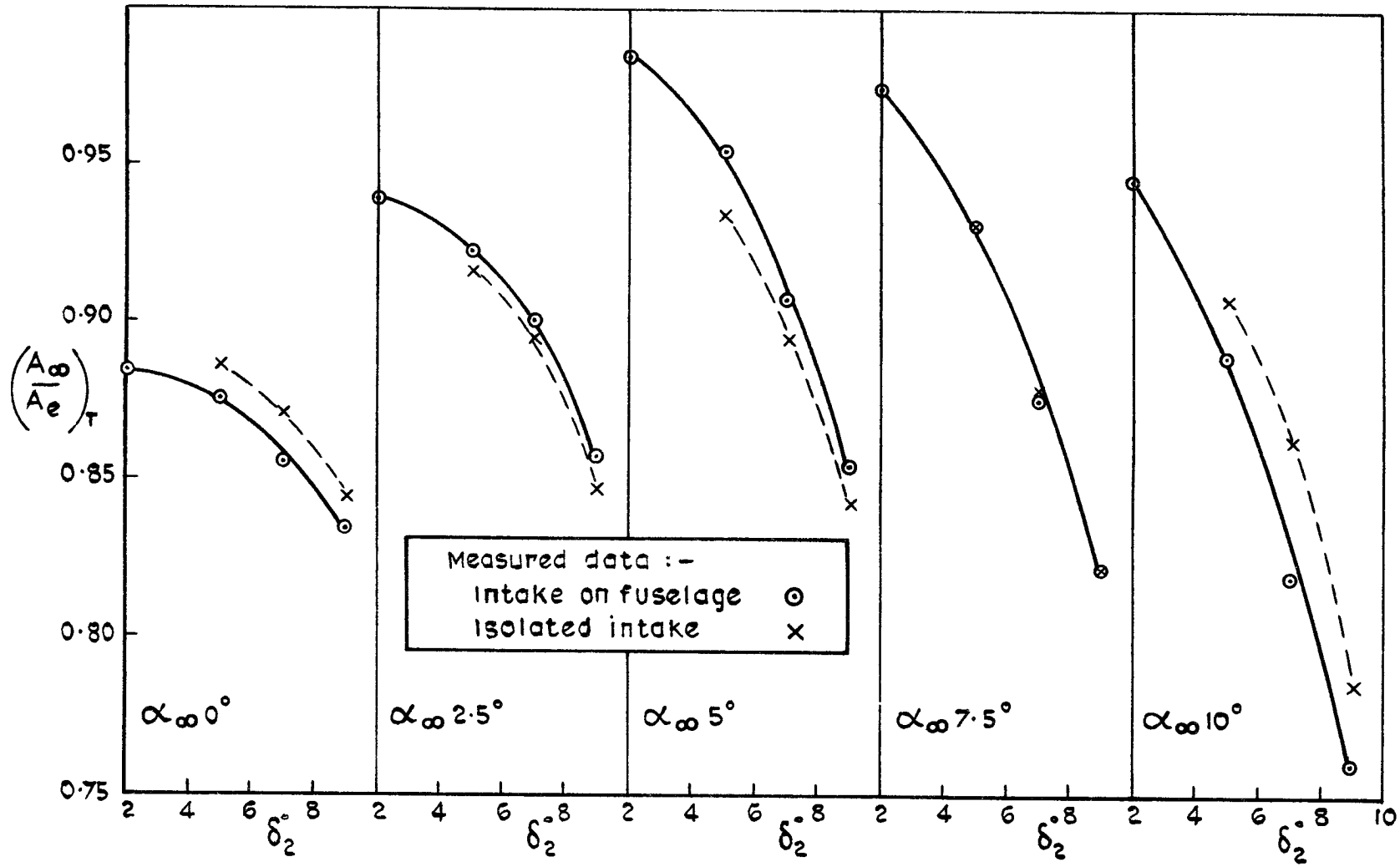

Fig.18 Maximum total mass flow ratio M_∞ 2·01

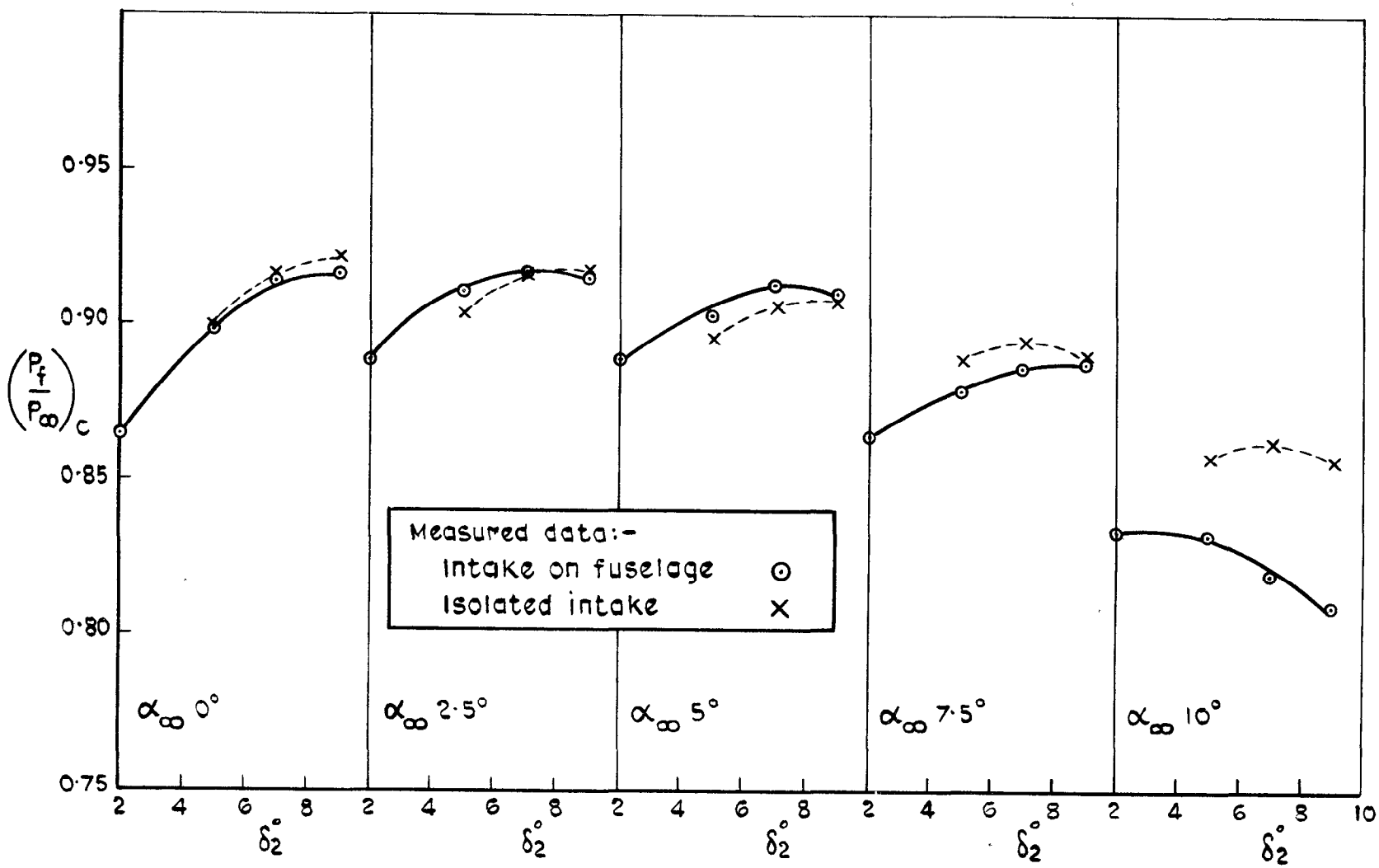

Fig.19 Pressure recovery at critical flow conditions M_∞ 2·01

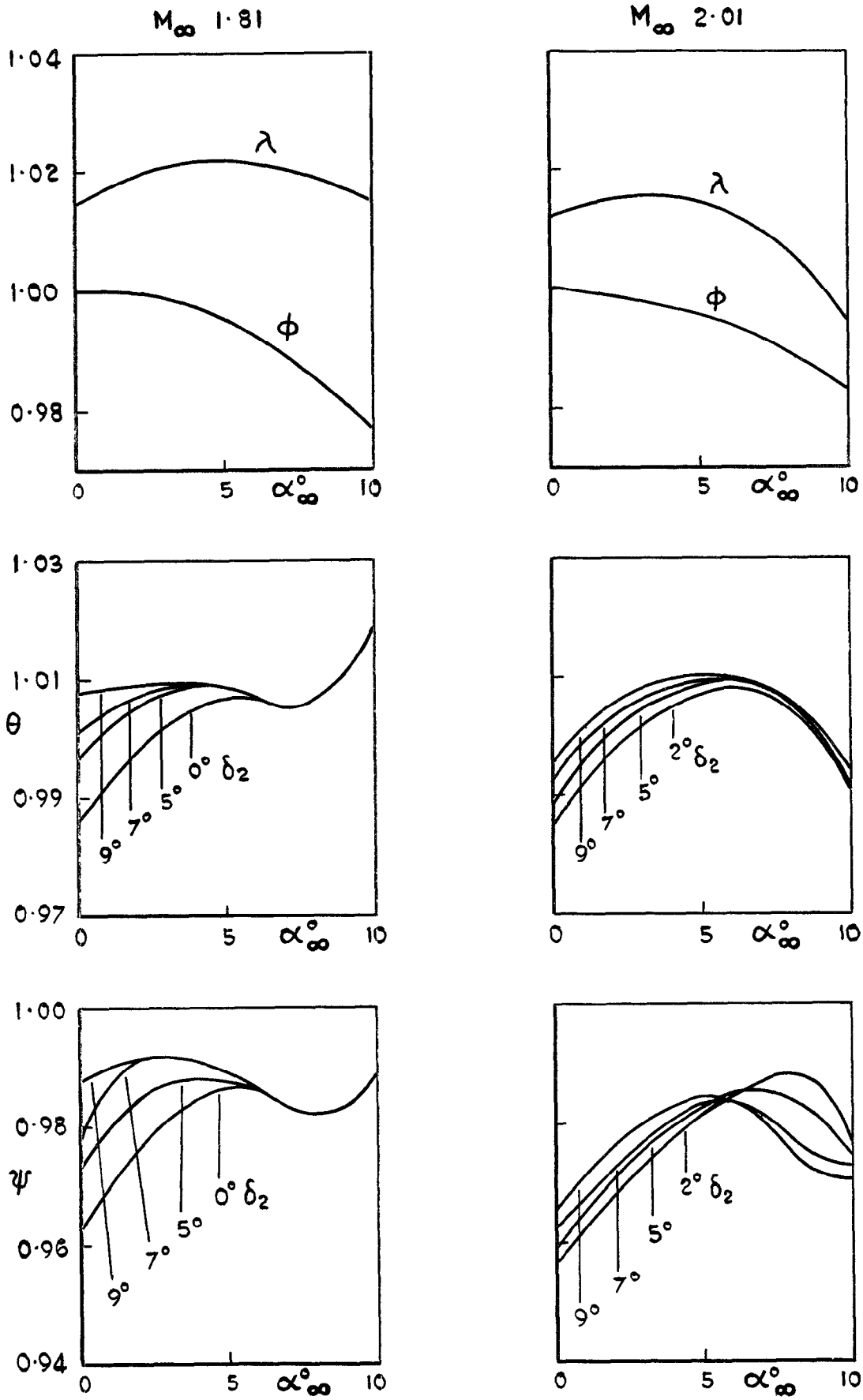

Fig. 20 Variation with incidence α_∞ of the parameters ϕ, λ, θ and ψ

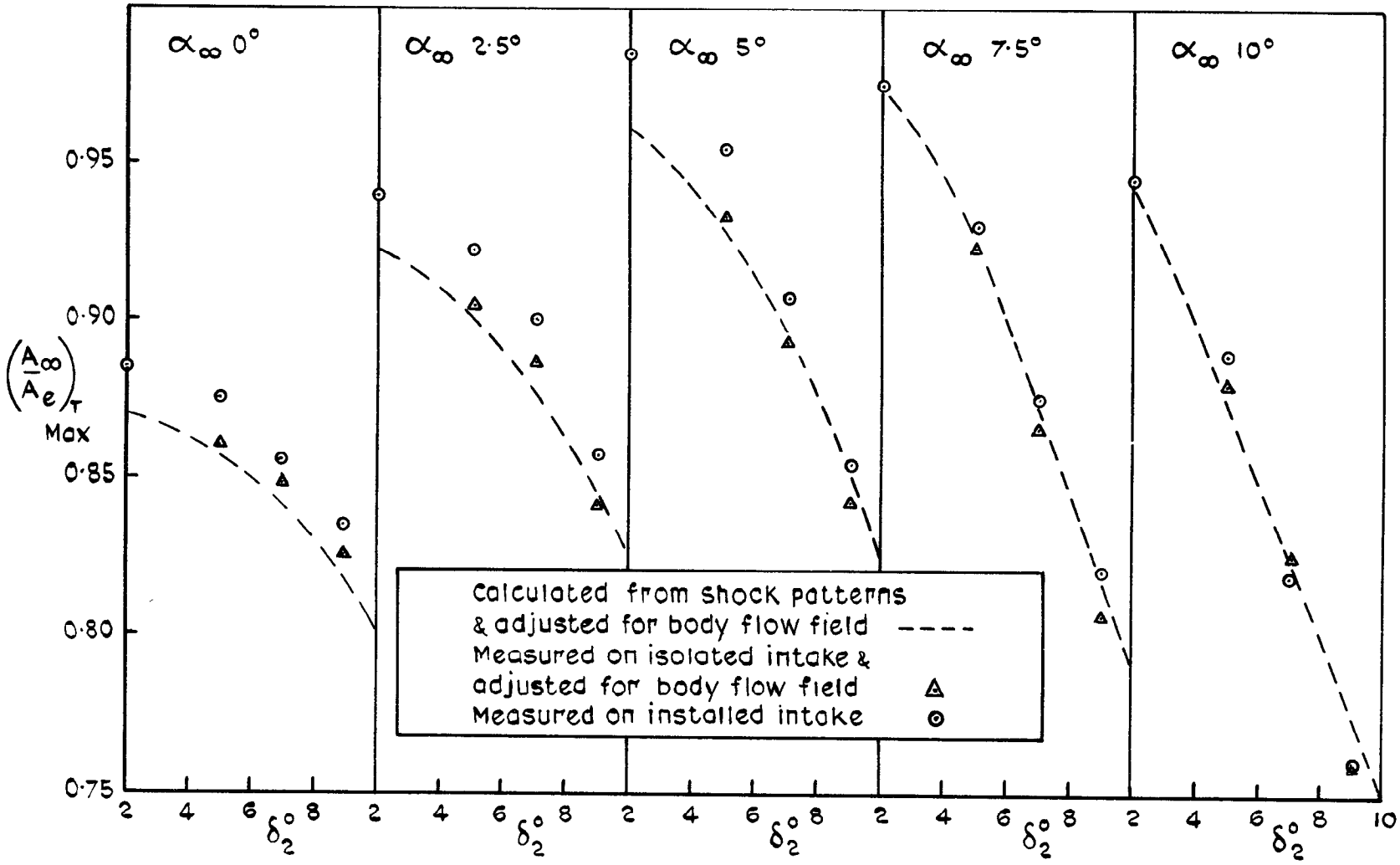

Fig. 21 Maximum total mass flow M_∞ 2·01

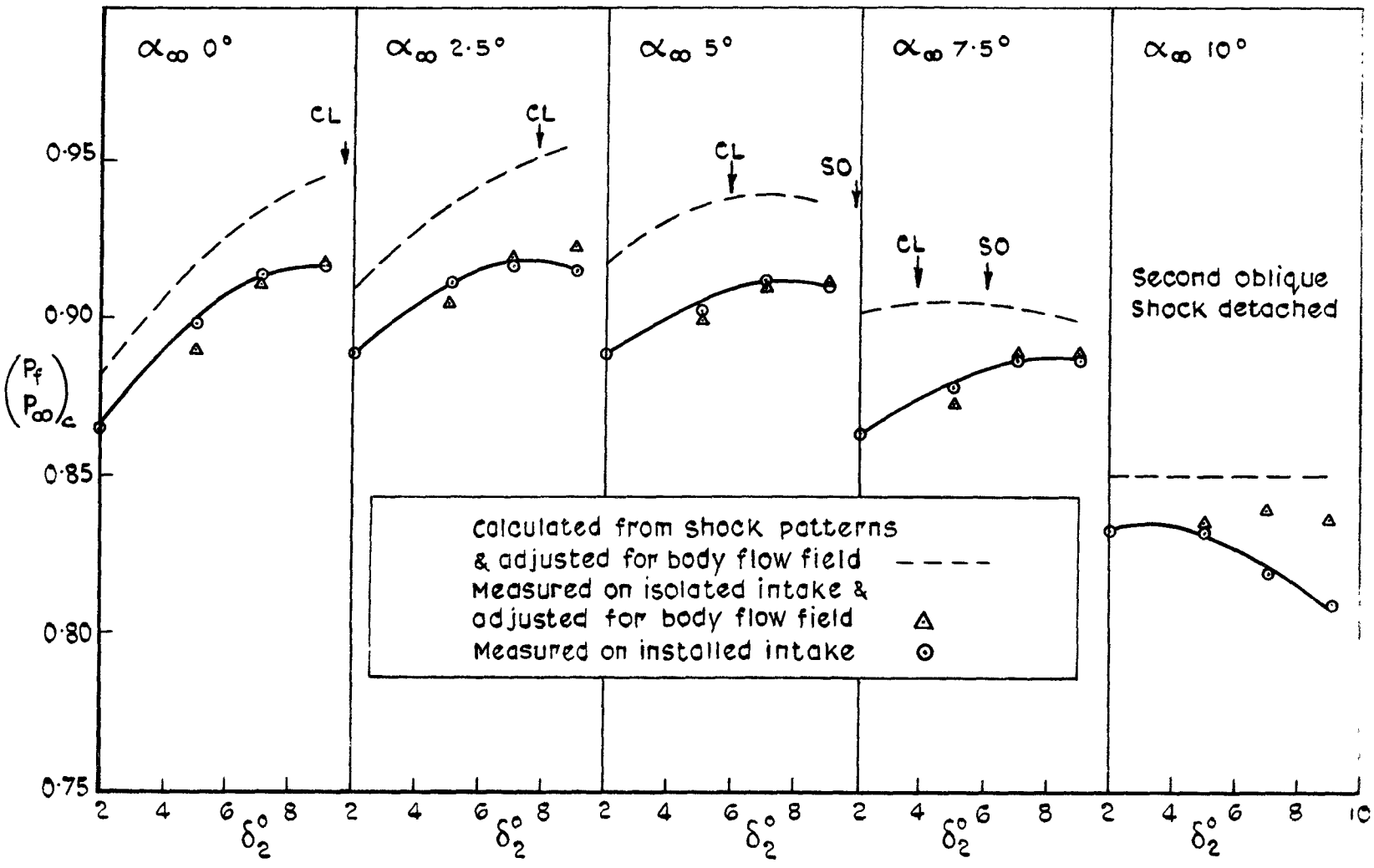

Fig. 22 Pressure recovery at critical flow conditions. M_∞ 2·01

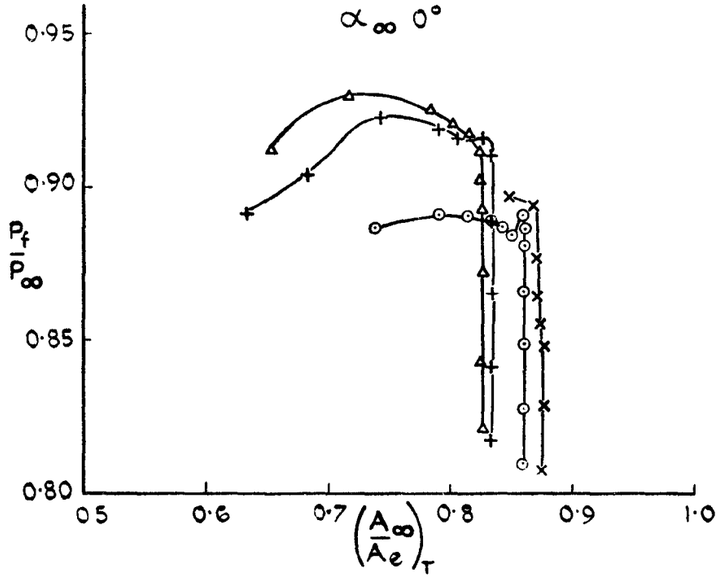

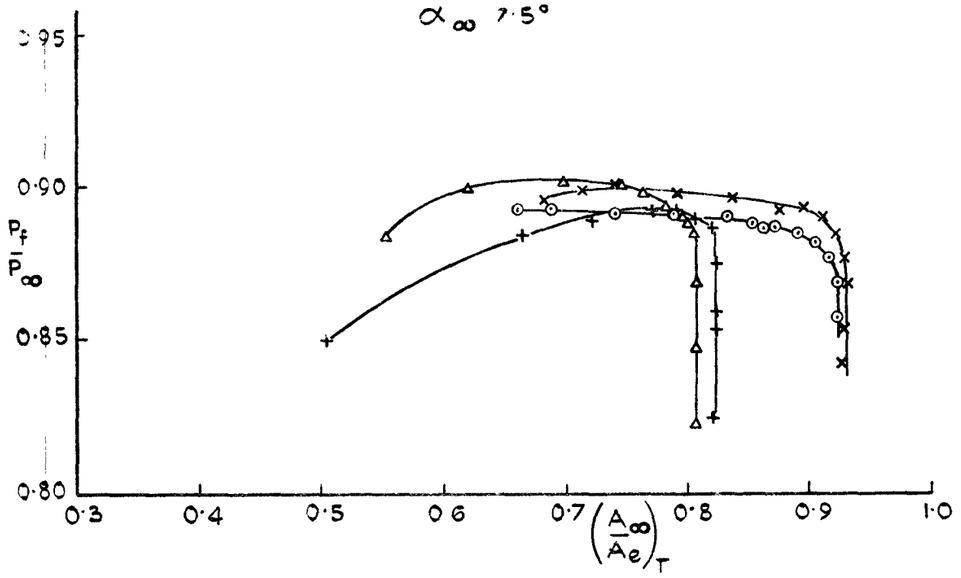

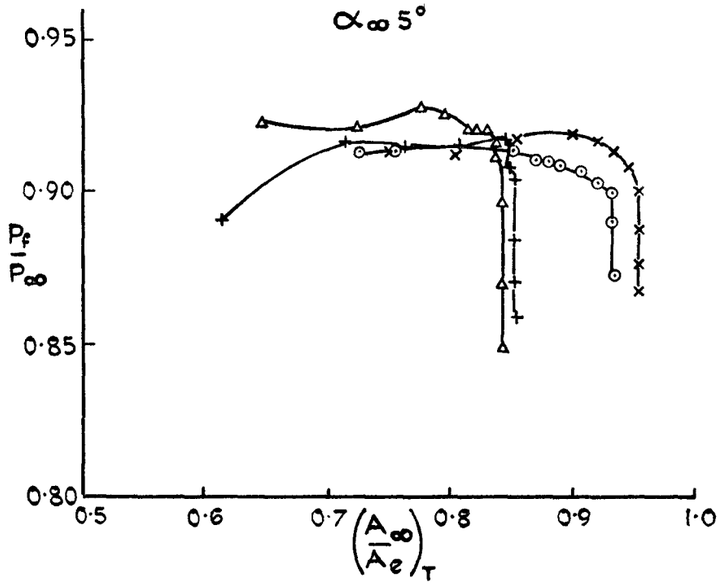

δ_2	5°	9°
Installed intake	×	+
Isolated intake adjusted for body flow field	⊙	△

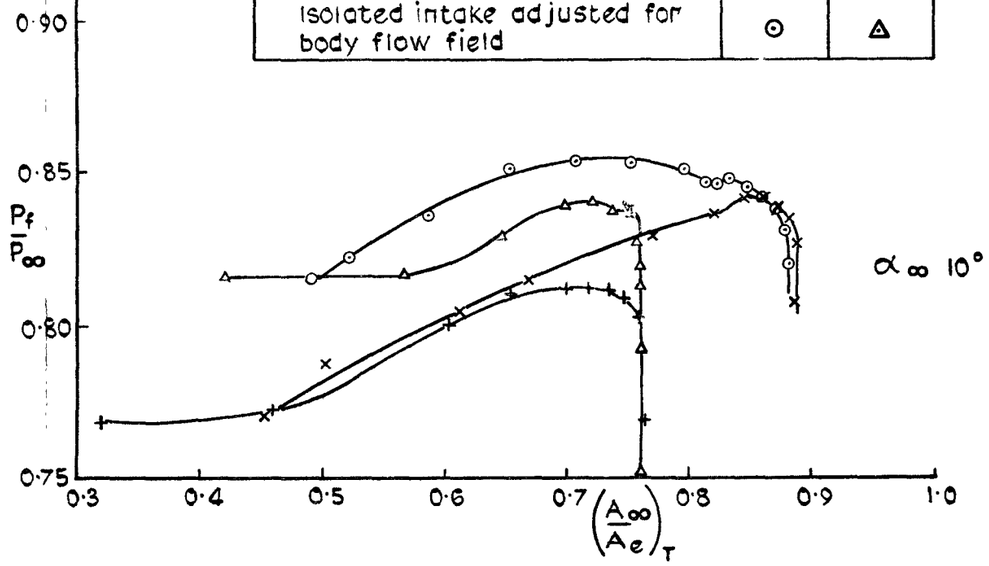

Fig. 23 Comparison of pressure recovery ~ mass flow characteristics for isolated & installed intake M_∞ 2·01

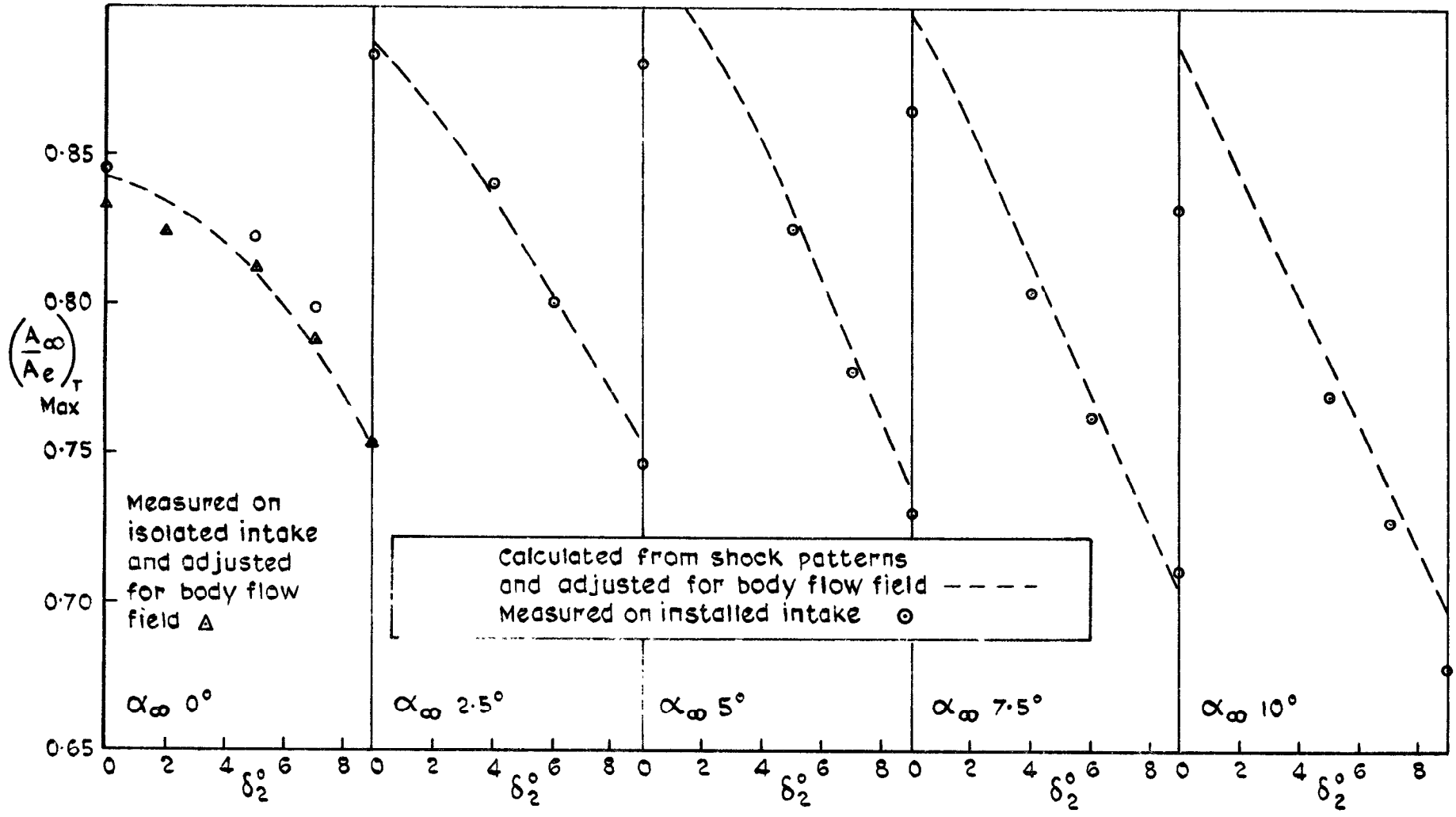

Fig.24 Maximum total mass flow M_∞ 1·81

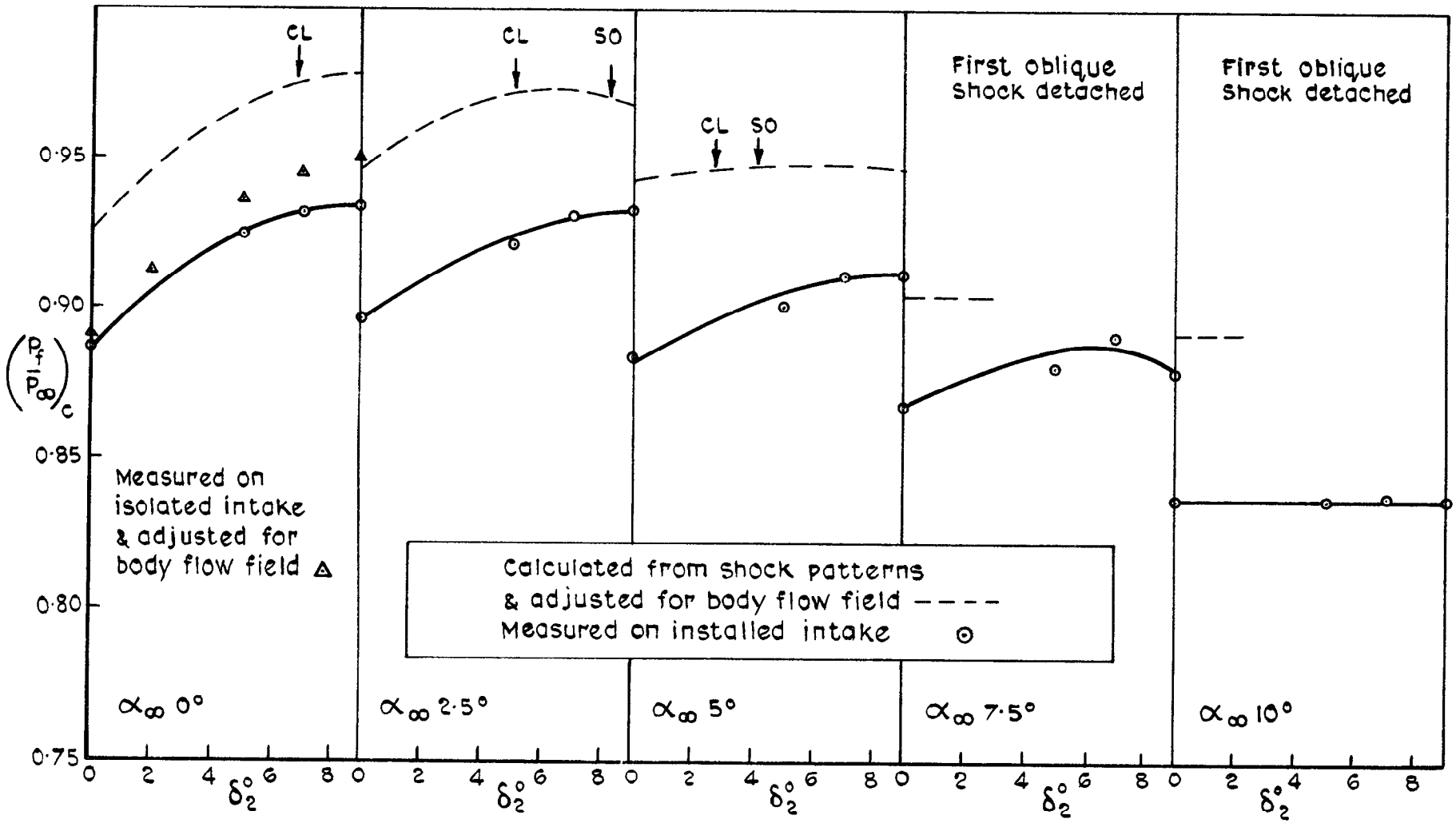

Fig. 25 Pressure recovery at critical flow conditions. M_∞ 1·81

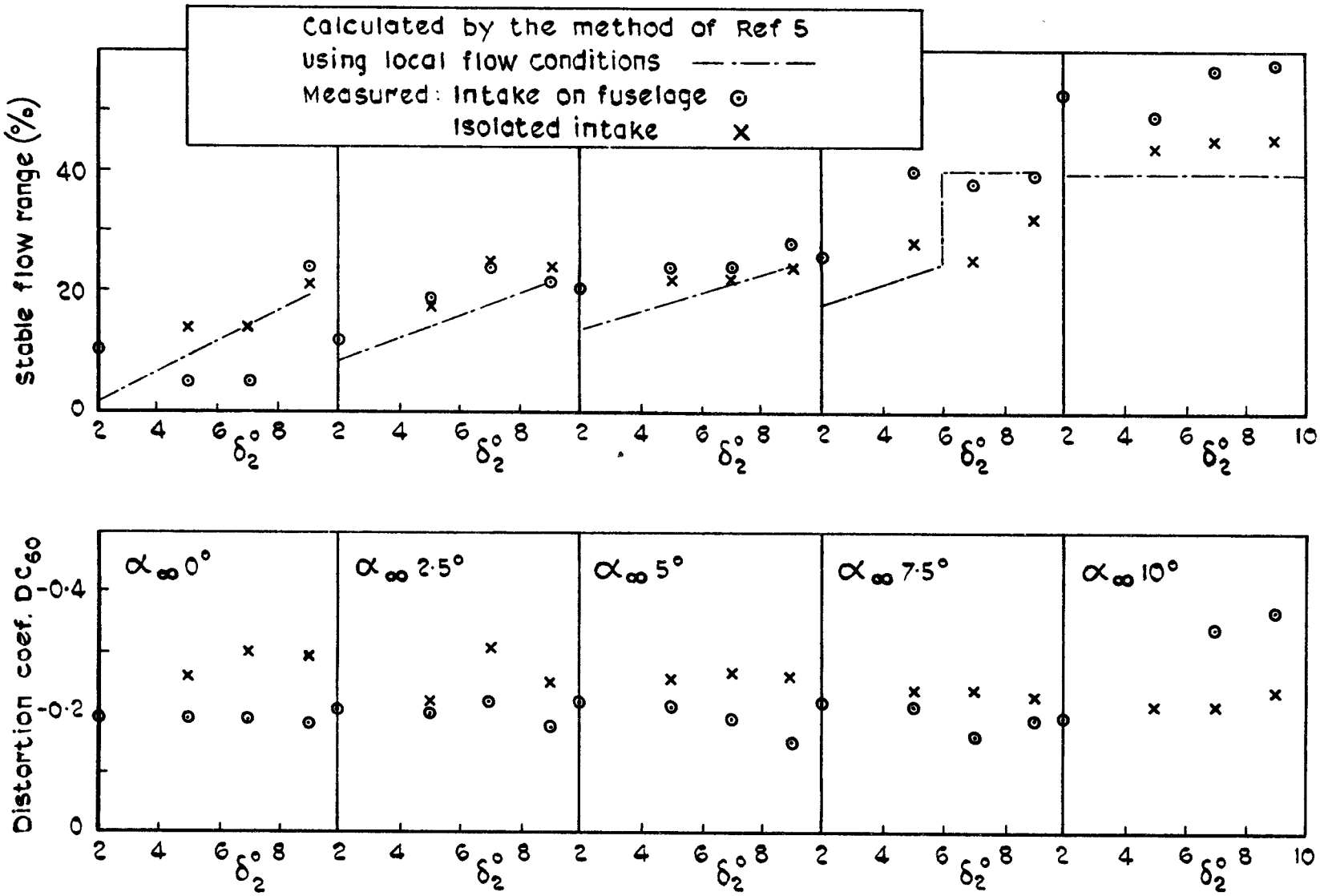

Fig. 26 Stable flow range & distortion coefficient DC_{60}
horizontal intake. M_∞ 2·01

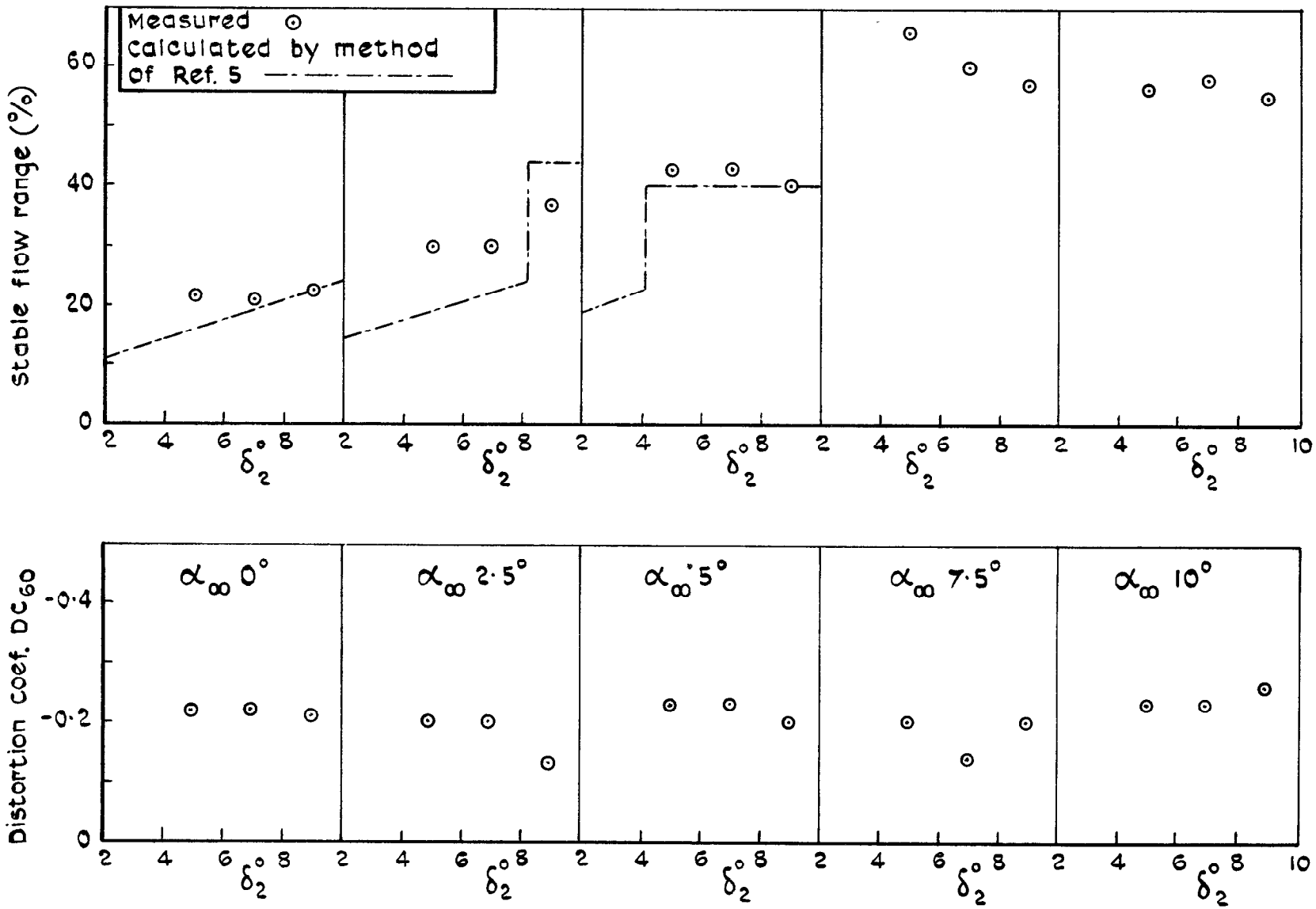

Fig.27 Stable flow range & distortion coefficient DC_{60} horizontal intake M_∞ 1·81

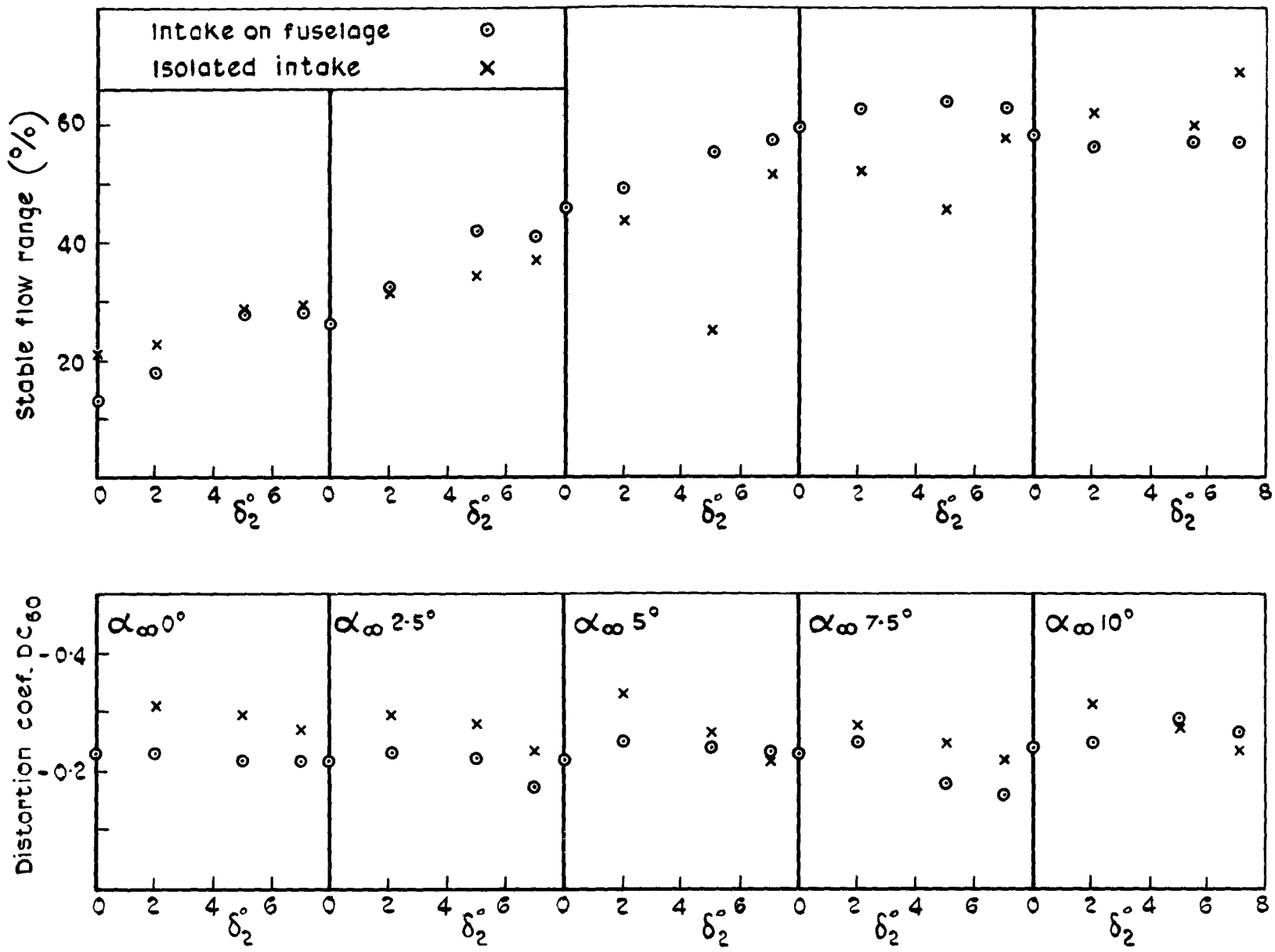

Fig. 28 Stable flow range & distortion coefficient DC_{60}
Horizontal intake $M_\infty = 1{\cdot}70$

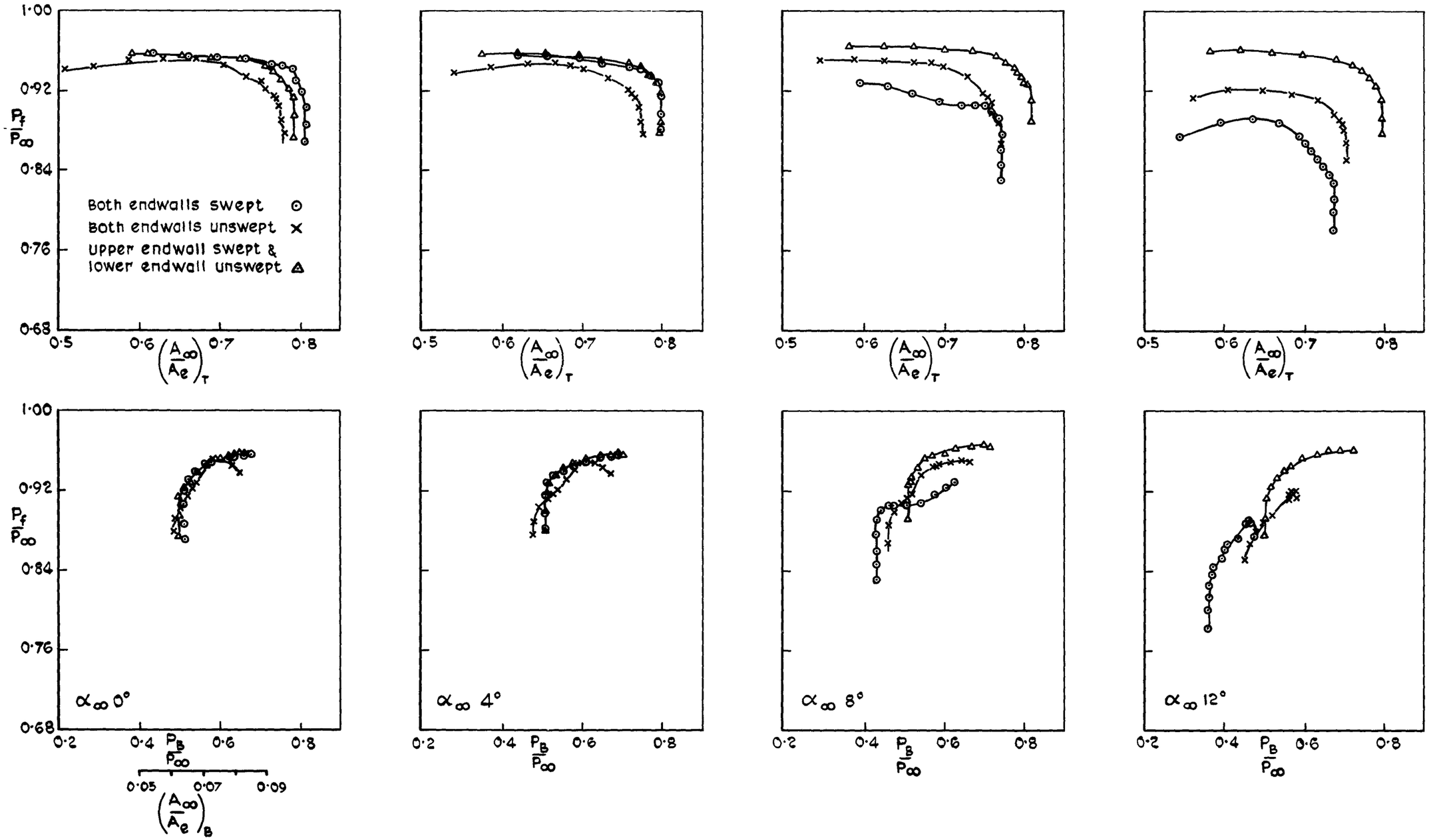

Fig. 29 Variation of engine face pressure recovery with total mass flow & bleed pressure recovery

Intake vertical M_∞ 1·61 δ_2 0°

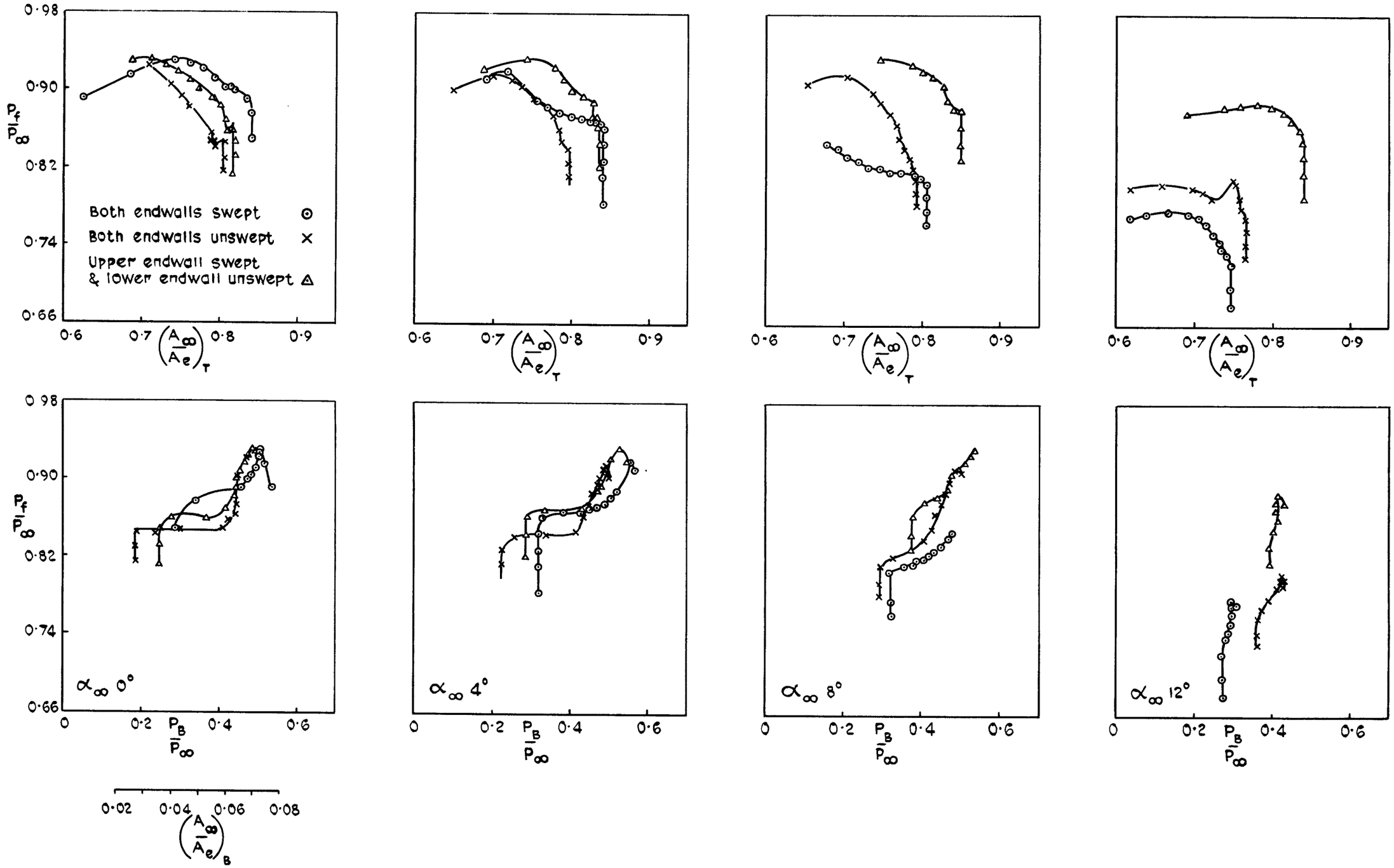

Fig. 30 Variation of engine face pressure recovery with total mass flow and bleed pressure recovery. Intake vertical M_∞ 1·81 δ_2 0°

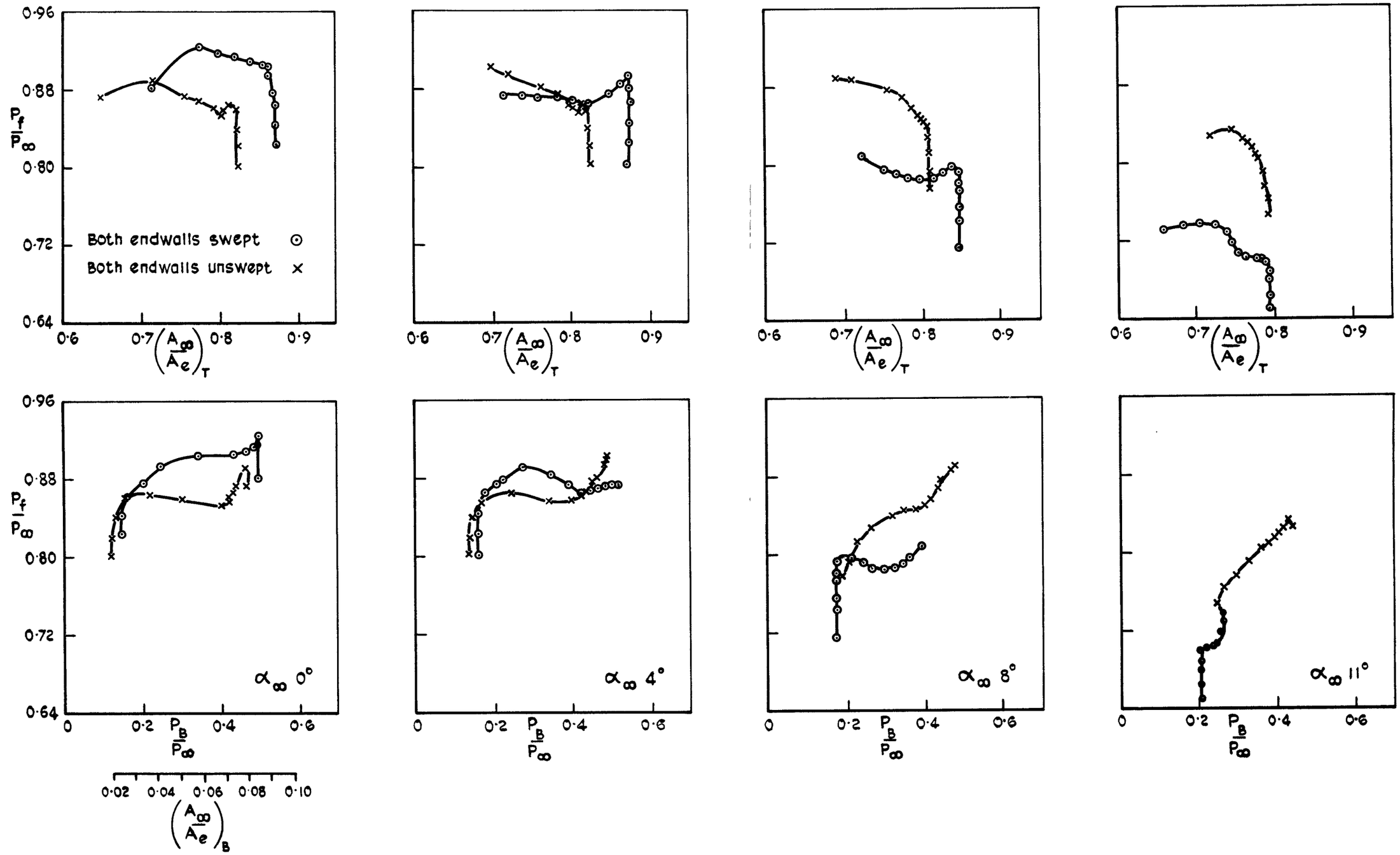

Fig.31 Variation of engine face pressure recovery with total mass flow and bleed pressure recovery
Intake vertical. M_∞ 2·01 δ_2 5°

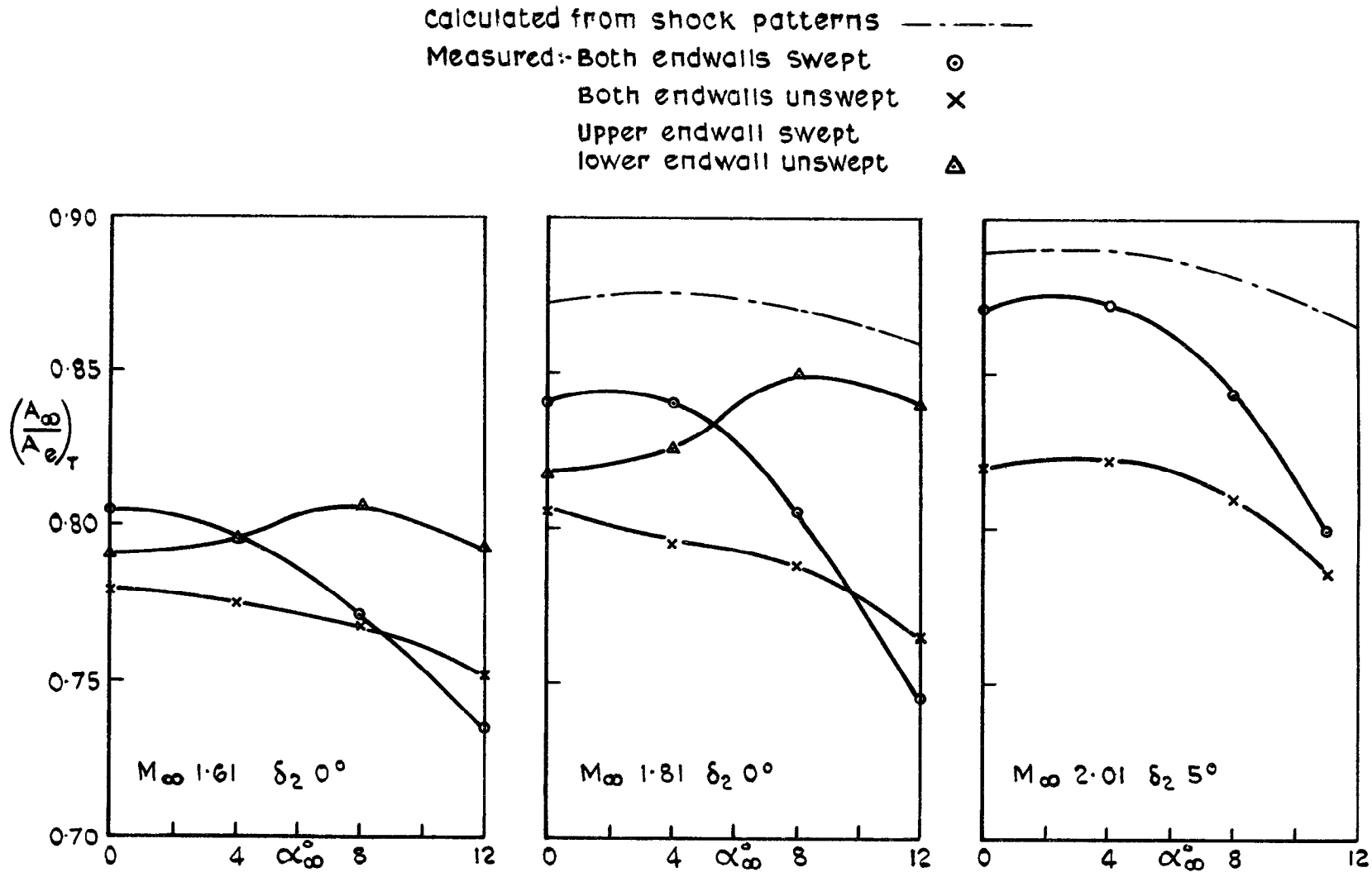

Fig.32 Variation of maximum total mass flow with incidence — intake vertical

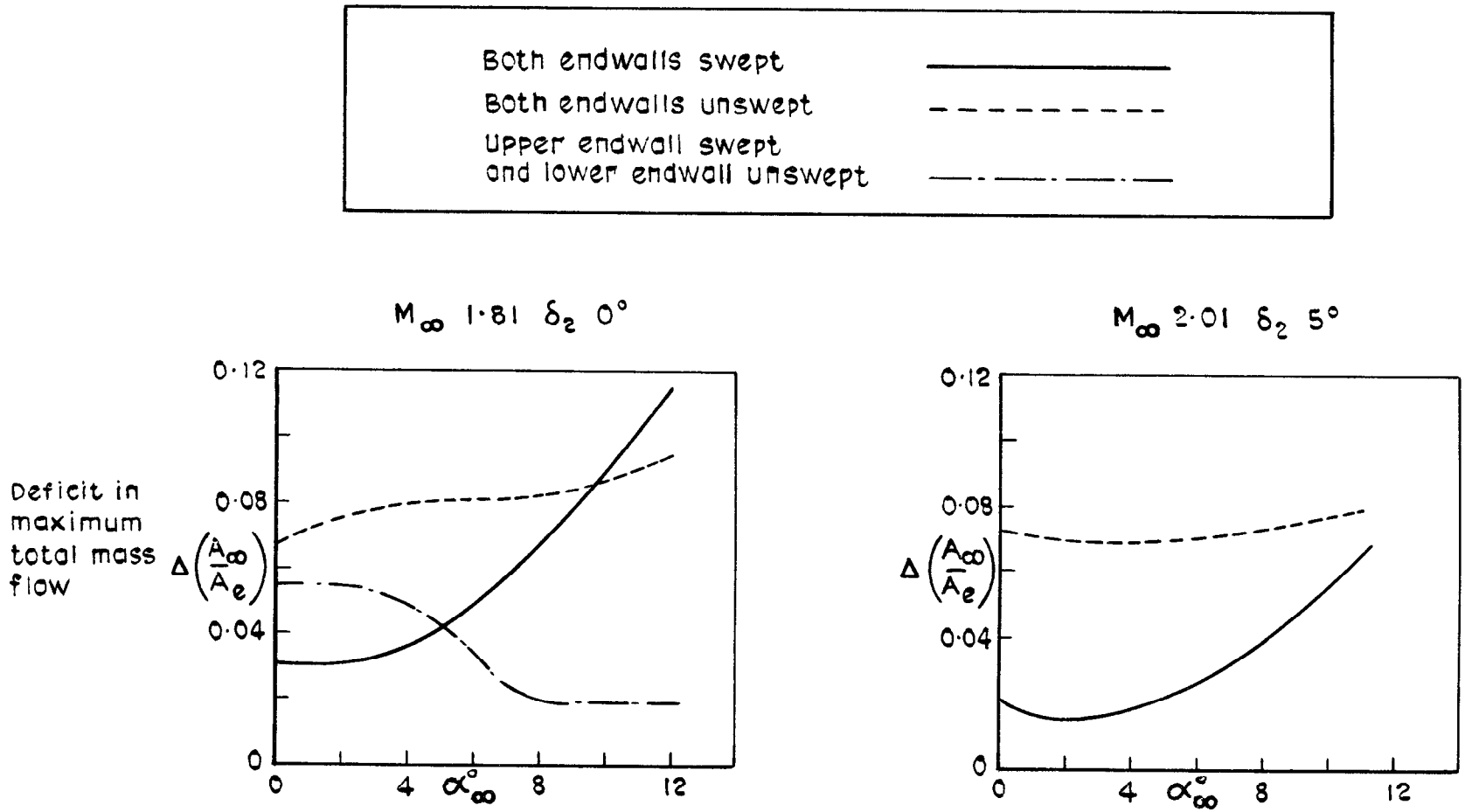

Fig. 33 Difference between calculated & measured maximum total mass flow – intake vertical

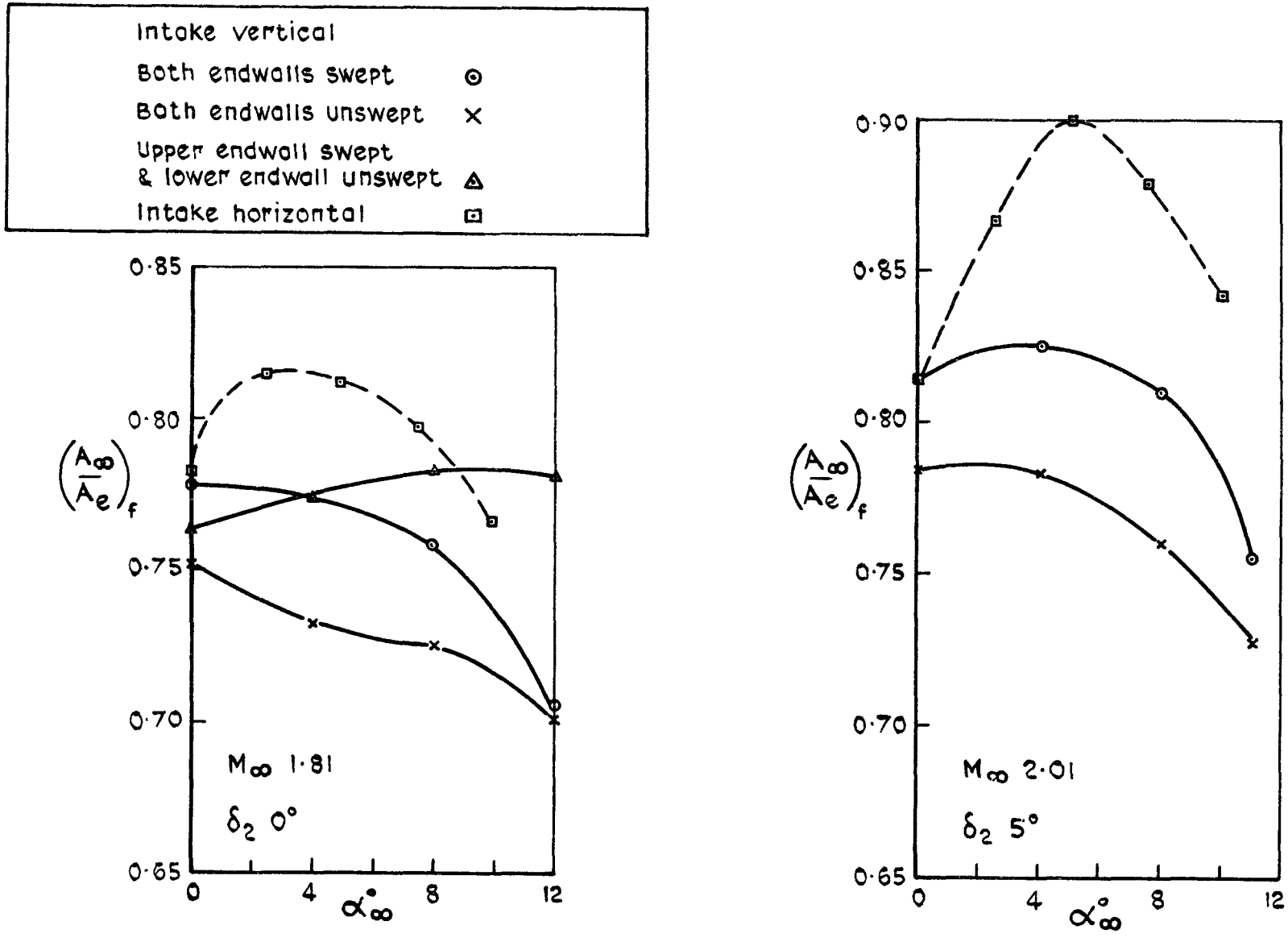

Fig. 34 Critical point engine face mass flow. Comparison between vertical and horizontal intakes

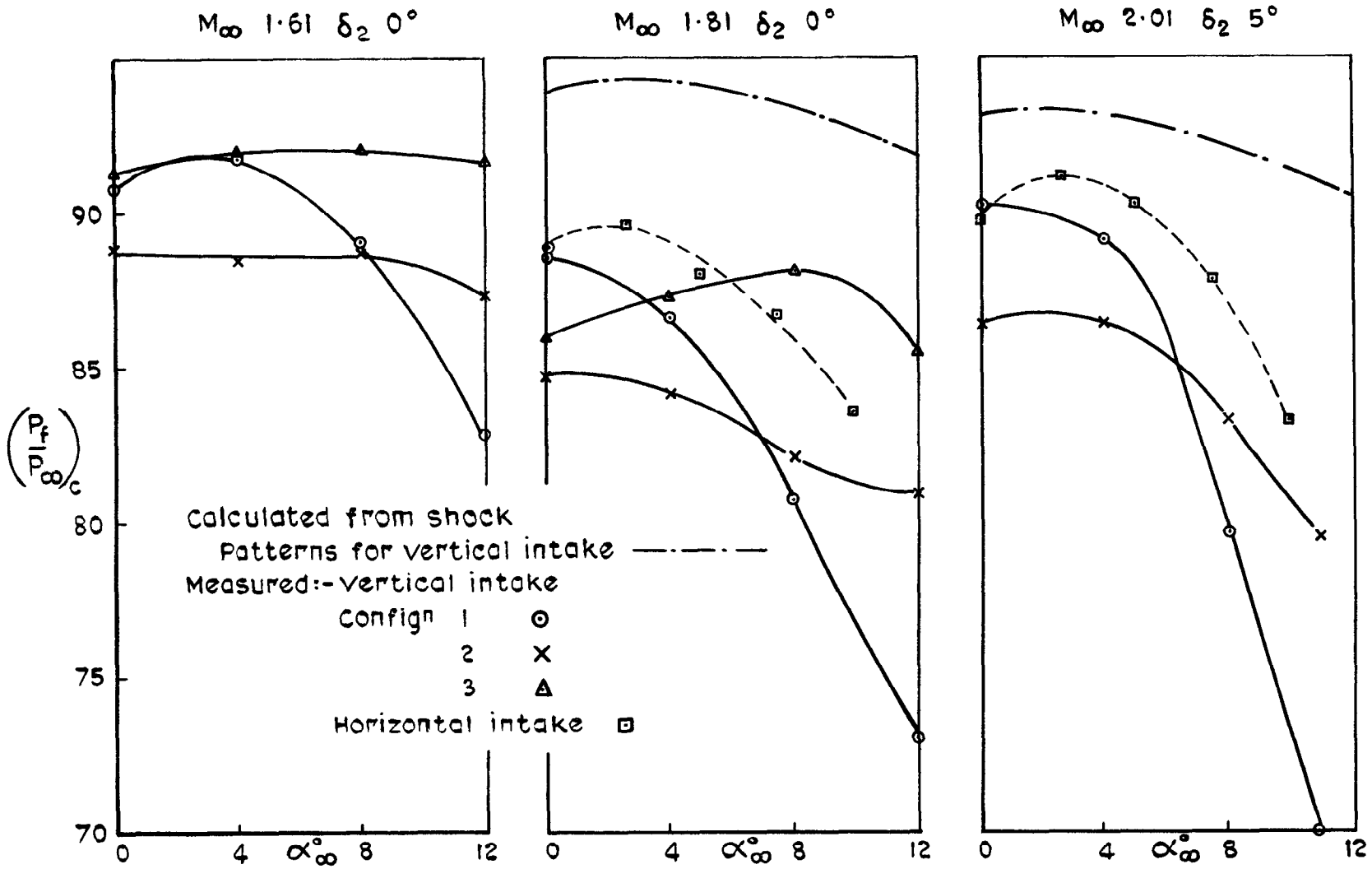

Fig. 35 Engine face pressure recovery at critical flow conditions (vertical & horizontal intakes)

These abstract cards are inserted in Technical Reports for the convenience of Librarians and others who need to maintain an Information Index.

Cut here

ARC CP No.1291
June 1972

Brown, C. S.
Goldsmith, E. L.

533.697.2 :
533.6.015 :
533.6.011.5 :
533.695.29

MEASUREMENT OF THE INTERNAL PERFORMANCE OF A RECTANGULAR AIR INTAKE MOUNTED ON A FUSELAGE AT MACH NUMBERS FROM 1.6 TO 2 – Part IV

A rectangular variable geometry intake, whose internal performance in a uniform flow field had previously been measured, has been tested on a fuselage. The intake has been tested with its leading edge both horizontal and vertical. In the case of the vertical intake, the effect of removing the lower swept endwall has been investigated.

The tests were done in a range of Mach number from 1.61 to 2.01 at incidences from 0^{o} to 12^{o}. The Reynolds number based on intake entry height was approximately 0.7×10^{6}.

(Over)

Cut here

ARC CP No.1291
June 1972

Brown, C. S.
Goldsmith, E. L.

533.697.2 :
533.6.015 :
533.6.011.5 :
533.695.29

MEASUREMENT OF THE INTERNAL PERFORMANCE OF A RECTANGULAR AIR INTAKE MOUNTED ON A FUSELAGE AT MACH NUMBERS FROM 1.6 TO 2 – Part IV

A rectangular variable geometry intake, whose internal performance in a uniform flow field had previously been measured, has been tested on a fuselage. The intake has been tested with its leading edge both horizontal and vertical. In the case of the vertical intake, the effect of removing the lower swept endwall has been investigated.

The tests were done in a range of Mach number from 1.61 to 2.01 at incidences from 0^{o} to 12^{o}. The Reynolds number based on intake entry height was approximately 0.7×10^{6}.

(Over)

DETACHABLE ABSTRACT CARDS

DETACHABLE ABSTRACT CARDS

This particular fuselage appears to impose only a small effect on the intake performance when the intake is horizontal. However a survey of the fuselage flow field indicates the complexity of the flow entering the intake and emphasizes the difficulty in using average flow properties to establish very accurate estimates of mass flow.

The vertical intake suffers considerable loss of performance both in terms of maximum mass flow and critical point pressure recovery at incidences above about 4^{o} when fitted with swept endwalls By removing the lower swept endwall, the zero incidence performance can be maintained up to incidences of 12^{o}.

This particular fuselage appears to impose only a small effect on the intake performance when the intake is horizontal. However a survey of the fuselage flow field indicates the complexity of the flow entering the intake and emphasizes the difficulty in using average flow properties to establish very accurate estimates of mass flow.

The vertical intake suffers considerable loss of performance both in terms of maximum mass flow and critical point pressure recovery at incidences above about 4^{o} when fitted with swept endwalls. By removing the lower swept endwall, the zero incidence performance can be maintained up to incidences of 12^{o}.

This particular fuselage appears to impose only a small effect on the intake performance when the intake is horizontal. However a survey of the fuselage flow field indicates the complexity of the flow entering the intake and emphasizes the difficulty in using average flow properties to establish very accurate estimates of mass flow.

The vertical intake suffers considerable loss of performance both in terms of maximum mass flow and critical point pressure recovery at incidences above about 4^{o} when fitted with swept endwalls. By removing the lower swept endwall, the zero incidence performance can be maintained up to incidences of 12^{o}.

© *Crown copyright* *1974*

Published by
HER MAJESTY'S STATIONERY OFFICE

To be purchased from
49 High Holborn, London WC1V 6HB
13a Castle Street, Edinburgh EH2 3AR
41 The Hayes, Cardiff CF1 1JW
Brazennose Street, Manchester M60 8AS
Southey House, Wine Street, Bristol BS1 2BQ
258 Broad Street, Birmingham B1 2HE
80 Chichester Street, Belfast BT1 4JY
or through booksellers

C.P. No. 1291

ISBN 011 470875 4